Student thesis series INES nr 784

Assessing the effectiveness of *Spartina alterniflora* control in Dafeng Milu National Nature Reserve (2022–2025) using satellite imagery from Sentinel-2

Yang Hu

2026
Department of
Earth and Environmental Sciences
Lund University
Sölvegatan 12
S-223 62 Lund
Sweden

Yang Hu (2026).

Assessing the effectiveness of Spartina alterniflora control in Dafeng Milu National Nature Reserve (2022–2025) using satellite imagery from Sentinel-2

Master degree thesis, 30 credits in *GIS and Remote Sensing*
Department of Earth and Environmental Sciences, Lund University

Level: Master of Science (MSc)

Course duration: *January* 2026 until *June* 2026

Assessing the effectiveness of *Spartina alterniflora* control in Dafeng Milu National Nature Reserve (2022–2025) using satellite imagery from Sentinel-2

Yang Hu

Master thesis, 30 credits, in *GIS and Remote Sensing*

Zheng Duan
Department of Earth and Environmental Sciences, Lund University

Thesis evaluator:
Wenxin Zhang
Department of Earth and Environmental Sciences, Lund University

Course examiner:
Martin Berggren

Acknowledgements

I would like to express my sincere gratitude to my supervisor, Zheng Duan, for his invaluable guidance and insightful comments throughout my thesis work. His expertise and patience greatly shaped this research and helped me grow academically. I also thank my examiner, Wenxin Zhang, for his thoughtful feedback and constructive suggestions on my project plan and half-time report, which significantly improved the clarity and direction of this study.

Moreover, I would like to acknowledge the organizations and platforms that supported this research, including the European Space Agency (ESA), Google Earth Engine, the World Database on Protected Areas (WDPA), Google Earth, Esri, and the developers of the CM-SSM 2020 and S2Coast-2023 datasets. I would also like to thank Lund University for providing an excellent academic environment and the resources necessary for completing this research.

Finally, I am deeply grateful to my family and friends for their constant support and encouragement throughout my years of study abroad. Their care and encouragement have been an important source of motivation during this journey.

Declaration of AI tool use

In this thesis, I used generative AI tools only as a support for language polishing and code debugging. I retained full responsibility for the intellectual content, analysis, interpretation, and conclusions of this work.

All AI-assisted content was carefully reviewed, revised, and approved by me before inclusion in the thesis.

Abstract

Spartina alterniflora is a highly invasive plant that has extensively colonized Chinese coastal wetlands, degrading critical habitat for migratory waterbirds. In response, the Chinese government launched the Special Action Plan for *Spartina alterniflora* Prevention and Control (2022–2025), aiming to remove over 90% of the invaded area nationwide. This study quantitatively assessed the effectiveness of this campaign in Dafeng Milu National Nature Reserve (DMNNR), a UNESCO World Heritage site on the Yellow Sea coast, using satellite imagery from Sentinel-2 and a dual-method framework combining Random Forest (RF) classification with *Spartina alterniflora* Index (SAI) threshold extraction. Cloud-free Sentinel-2 scenes from December 2022 and December 2025 were analyzed to map *S. alterniflora* distribution before and after control. A total of 640 reference samples were collected through multi-source image interpretation and split spatially into a western subset for training and eastern subset for independent testing, which were used to train an RF classifier and derive site-specific SAI thresholds ($-0.790 \leq \text{SAI} \leq -0.388$). The RF model achieved an overall accuracy of 94.97% on the independent test set. High spatial agreement between the RF-based and SAI-based maps, quantified by the Intersection over Union (IoU = 0.916) validated the SAI approach, which was applied to 2025 imagery for sample-free remnant patch detection. Results show that the invaded area declined from 3,147.86 ha to 22.84 ha, representing a 99.27% removal rate that substantially exceeds the 90% national target. Of the baseline extent, 3,141.92 ha (99.81%) was cleared, with only 5.95 ha persisting and 16.89 ha of new growth detected. Remnant patches exhibited strong spatial clustering (Moran's I = 0.95, $p < 0.001$) in three hotspots along the seaward fringe. The complete disappearance of *S. alterniflora* spectral signatures in SAI and NDVI histograms confirmed large-scale removal attributable to the management. The restoration of over 3,000 ha of tidal flat supports UNESCO conservation objectives and maintains critical foraging habitat for globally threatened shorebirds. The transferable dual-method framework addresses key limitations in post-eradication monitoring where field access is constrained, providing a practical tool for evaluating control effectiveness across coastal reserves.

Keywords: Geographical Information Science, Remote Sensing, *Spartina alterniflora*, invasive species control, Sentinel-2, coastal wetlands, Random Forest

Table of contents

Acknowledgements ii

Declaration of AI tool use ii

Abstract iii

Table of contents iv

1. Introduction 1

2. Background 4

  2.1. *Spartina alterniflora* invasion and management in China 4

  2.2. Ecological importance of the Yellow Sea tidal flats and DMNNR 5

  2.3. Remote sensing of *Spartina alterniflora* 7

  2.4. Methods for mapping *Spartina alterniflora*: Random Forest and SAI 8

  2.5. Conceptual framework 9

3. Methodology 10

  3.1. Study area 10

  3.2. Data 12

    3.2.1. Sentinel-2 imagery 12

    3.2.2. S2Coast-2023 coastline dataset 14

    3.2.3. Ancillary data 15

  3.3. Method 17

    3.3.1. Land Cover Composition Analysis 17

    3.3.2. Sample Collection 19

    3.3.3. Random Forest Classification 21

    3.3.4. SAI Threshold Extraction 23

    3.3.5. Spectral Distribution Analysis 24

    3.3.6. Change Analysis 24

    3.3.7. Spatial Pattern Analysis of Persistent Patches 25

4. Results 26

  4.1. Land Cover Composition 26

  4.2. SAI Threshold Determination 27

  4.3. RF Classification and SAI Extraction Comparison in 2022 29

  4.4. Spectral Distribution Analysis 32

  4.5. Change Analysis 34

4.6. Spatial Pattern Analysis of Persistent Patches 36
5. Discussion 38
5.1. Control Effectiveness 38
5.2. Residual Patches 39
5.3. Methodological Strengths and Reliability 40
5.3.1. Complementarity of RF and SAI Methods 40
5.3.2. Applicability of SAI Threshold in 2025 41
5.3.3. Attribution of Change to Management Actions 41
5.4. Limitations of this study 42
5.4.1. Lack of independent field validation for 2022 baseline 42
5.4.2. Absence of independent validation for 2025 43
5.5. Implications for Future Monitoring and Management 43
6. Conclusions 44
References 47

1. Introduction

Spartina alterniflora is widely recognized as one of the most problematic invasive plants in coastal wetlands worldwide (Zheng et al., 2023). It forms dense monospecific stands that outcompete native saltmarsh vegetation, alter tidal hydrodynamics, trap sediments and reduce the quality of foraging habitat for migratory shorebirds (Lee, 2013). In China, *S. alterniflora* was deliberately introduced in 1979 for coastal protection and land reclamation (Ma et al., 2023), but it has since spread rapidly along large parts of the coastline and become a major ecological threat in several key wetland reserves (Zuo et al., 2025).

To address this problem, the Chinese government launched the "Special Action Plan for *Spartina alterniflora* Prevention and Control (2022–2025)", which aims to remove more than 90% of the invaded area at the national scale (Wetland Management Department Circular No. 132). This large-scale campaign represents an unprecedented management effort, but its real ecological effectiveness is still poorly quantified at the level of individual protected areas. In particular, there is limited evidence on how much *S. alterniflora* has actually been cleared, where remnant patches persist, and whether these remaining stands show spatial clustering that may increase the risk of reinvasion.

Dafeng Milu National Nature Reserve (DMNNR), located on the Yellow Sea coast of Jiangsu Province, is one of the most ecologically important coastal wetlands in China (Fig. 1). It forms part of the UNESCO World Natural Heritage site "Migratory Bird Sanctuaries along the Coast of Yellow Sea and Bohai Gulf of China" (UNESCO, 2019) and provides important stopover and wintering habitat for many globally threatened shorebird and waterbird species. At the same time, the intertidal flats of DMNNR have experienced extensive invasion by *S. alterniflora* (Yan et al., 2021) and have been a priority area in the national control campaign.

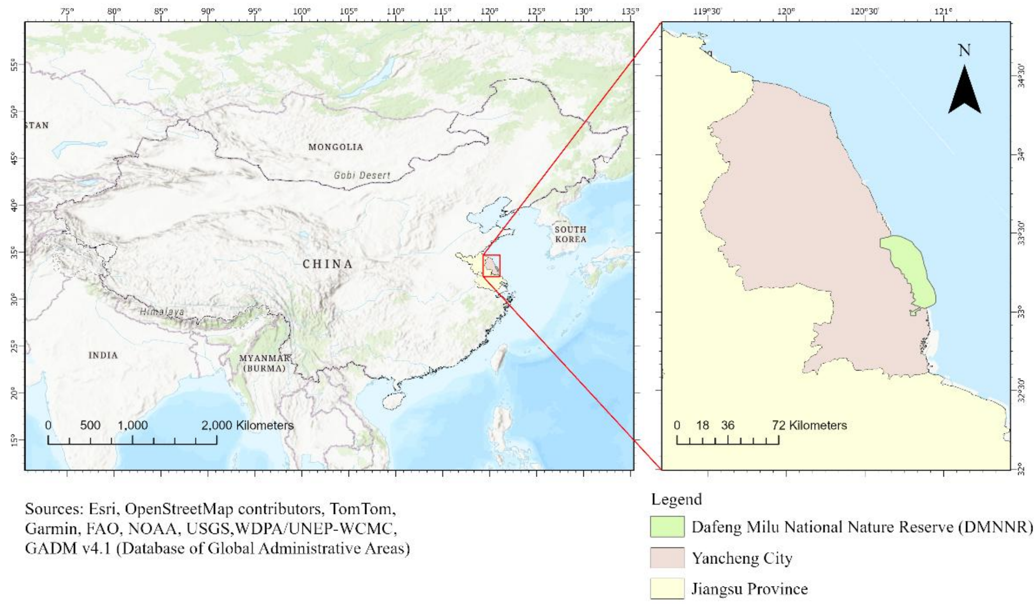

Fig. 1. Location of the Dafeng Milu National Nature Reserve (DMNNR) along the Yellow Sea coast of Jiangsu Province, eastern China. The left map shows the overall geographic position of Jiangsu Province within China, while the right enlarged map delineates the administrative scope of Jiangsu Province, Yancheng City, and the boundary of Dafeng Milu National Nature Reserve.

Given the global conservation value of DMNNR and its central role in the Yellow Sea flyway, it is crucial to evaluate whether the 2022–2025 control efforts have effectively restored the intertidal zone by removing *S. alterniflora*. However, previous studies in this region have mainly focused on long-term expansion and dieback patterns using Landsat time series, and few have assessed the short-term outcomes of the recent nationwide eradication program using higher-resolution satellite data.

Satellite remote sensing provides an efficient tool for monitoring coastal vegetation over large and dynamic intertidal areas that are difficult to access in the field (Davies et al., 2023). Sentinel-2 imagery, in particular, offers 10 m spatial resolution, frequent revisit and several red-edge bands that have proven useful for mapping *S. alterniflora* (Dong et al., 2024; Liu et al., 2025). Zuo et al. (2025) have further proposed the *Spartina alterniflora* Index (SAI), a simple spectral index that enables sample-free extraction of *S. alterniflora* during its senescence period. Building on these developments, this thesis combines SAI-based threshold extraction with Random Forest classification and spatial statistical analysis to assess the effectiveness of *S. alterniflora* control in DMNNR between 2022 and 2025.

Overall, *S. alterniflora* has experienced large-scale expansion and partial removal along the Chinese coast (Zhang et al., 2020; Liu et al., 2025). However, most of these studies have focused on invasion changes at the national or provincial scale, and there is still no clear quantitative evidence of how much area has been reduced and what proportion has been cleared in a single protected area such as DMNNR before and after the national campaign. In addition, previous assessments of *S. alterniflora* have usually used total area increase or decrease as the main indicator, and have rarely examined the distribution of cleared, persistent, and newly established patches within a region, making it difficult to identify potential high-risk areas after control (Zhang et al., 2020; Zhou et al., 2025).

To address these gaps, this study proposes a framework to quantitatively evaluate how the 2022–2025 national control campaign has changed the extent and spatial pattern of *S. alterniflora* in the intertidal zone of DMNNR by combining Sentinel-2 imagery with geospatial analyses implemented in Google Earth Engine and ArcGIS Pro. Specifically, the thesis addresses the following research questions:

RQ1: What were the spatial distribution patterns and total areas of *S. alterniflora* in the intertidal zone of DMNNR in 2022 and 2025?

RQ2: To what extent did large-scale management reduce *S. alterniflora* area between 2022 and 2025, in terms of net area change, eradication rate and the balance between cleared, persistent and newly established patches?

RQ3: Where are the persistent and newly grown *S. alterniflora* patches located, and do these remnant stands exhibit spatial clustering?

2. Background

2.1. *Spartina alterniflora* invasion and management in China

Spartina alterniflora is a perennial saltmarsh grass native to the Atlantic coasts of North and South America, but it has now become one of the most serious invasive plants in many coastal wetlands worldwide (Liu et al., 2020; Zheng et al., 2023). In China, the species was deliberately introduced from the United States in 1979 and was initially promoted for coastal defense, land reclamation and sediment trapping, because of its high tolerance to salinity, tidal inundation and unstable substrates (Ma et al., 2023; Chen et al., 2022). However, the ecological costs of this introduction soon became apparent. Its strong adaptation to high salinity and tidal disturbance, together with its ability to spread propagules via tidal currents, gave *S. alterniflora* a high capacity for survival and reproduction (Xia et al., 2021), allowing it to expand rapidly across the intertidal zones of many estuaries and coastal reserves and to form dense monospecific stands.

Since its introduction, *S. alterniflora* has spread widely across coastal wetlands along the mainland Chinese coast, spanning from 18°N to 41°N, covering coastal areas of Hebei, Tianjin, Shandong, Jiangsu, Shanghai, Zhejiang, Fujian, Guangdong and Guangxi (Zuo et al., 2025). By 2020, *S. alterniflora* had occupied about 626 km^2 of intertidal habitat in China, indicating that the invasion had reached a nationwide scale. The severity of invasion is not spatially uniform. Around 97% of the national distribution is concentrated in six coastal regions: Jiangsu, Zhejiang, Shanghai, Shandong, Fujian and Guangxi (Yan et al., 2021; Zhang et al., 2020). Among these, Jiangsu and Shanghai have long been recognized as invasion hotspots, mainly because of the extensive spread of *S. alterniflora* in the Yancheng wetlands and the Yangtze River estuary. Fujian and Zhejiang are also high-risk areas, especially where *S. alterniflora* overlaps spatially with mangrove forests and estuarine wetlands, posing additional threats to native vegetation and biodiversity conservation (Zheng et al., 2023).

Management of *S. alterniflora* in China did not begin only with the 2022–2025 national campaign. Before that, several local and regional control efforts had already been implemented, especially in ecologically sensitive reserves and estuarine wetlands. For example, on Chongming Island in the Yangtze estuary, large-scale ecological engineering projects were carried out: the area of *S. alterniflora* increased from about

4 ha in 1995 to around 2,067 ha in 2012, but then declined markedly after a major removal project implemented between 2013 and 2016 (Zhang et al., 2020). Nevertheless, a considerable remnant area still remained in 2018, suggesting that control can substantially reduce the invaded area but may not completely eliminate sources of reinvasion (Zhang et al., 2020). Early management efforts in China mainly relied on physical control methods, such as cutting, mowing, ploughing, rotary tilling and prolonged flooding, sometimes combined with embankments or enclosure measures (Min et al., 2025). However, in highly dynamic intertidal environments, they are often costly and difficult to implement efficiently (Min et al., 2025). Management successfully reduced the local invaded area, but persistent or newly established patches still remained after treatment, creating an ongoing risk of reinvasion (Zhang et al., 2020).

Against this background, the Chinese government launched the Special Action Plan for *Spartina alterniflora* Prevention and Control (2022–2025), which set a national target of eliminating more than 90% of *S. alterniflora* by the end of 2025 (National Forestry and Grassland Administration, 2022). This plan marks a shift from fragmented, local interventions towards more coordinated, province-scale and national-scale control (Min et al., 2025). Since 2021, and especially after 2022, coastal provinces have implemented large-scale eradication projects, with Shandong and Fujian among the earliest to launch regional comprehensive removal program (Min et al., 2025). Under this new management context, reliable monitoring is needed not only to quantify total removal, but also to locate remnant patches and to identify priority areas for follow-up control (Zuo et al., 2025).

2.2. Ecological importance of the Yellow Sea tidal flats and DMNNR

The Yellow Sea region contains an extensive belt of intertidal mudflats that stretches along the coasts of China, the Democratic People's Republic of Korea and the Republic of Korea (UNESCO, 2019). These wide tidal flats form a key part of the East Asian–Australasian Flyway (EAAF), providing staging and wintering habitats where large numbers of migratory shorebirds and waterbirds can rest and refuel during long-distance journeys (Chan et al., 2019). Because many EAAF populations depend on this limited stretch of coastline, the Yellow Sea–Bohai Gulf is often regarded as a bottleneck area: loss or degradation of intertidal habitats in this region can have disproportionate negative impacts on global shorebird populations (UNESCO, 2019; Mu & Wilcove, 2020).

In recognition of this exceptional ecological value, the serial property "Migratory Bird Sanctuaries along the Coast of Yellow Sea–Bohai Gulf of China (Phase I)" was inscribed on the UNESCO World Heritage List in 2019 (UNESCO, 2019). The Phase I sites are located along the coast of Yancheng in Jiangsu Province and include extensive tidal flats, saltmarshes and associated wetlands that together provide habitat for more than 400 bird species, including many that are globally threatened.

Dafeng Milu National Nature Reserve (DMNNR) lies within this coastal zone and forms part of the core area of the World Heritage property (Yan et al., 2022). The reserve contains a mosaic of habitats, ranging from reclaimed land and artificial grassland to wide intertidal mudflats and saltmarshes seaward of the coastal seawall, and is internationally known both for supporting migratory waterbirds and for hosting a reintroduced population of Père David's deer (*Elaphurus davidianus*) (Yan et al., 2022; Ma et al., 2023). The intertidal zone of DMNNR provides crucial feeding and roosting sites for shorebirds and other waterbirds, which rely on exposed mudflats and shallow tidal creeks to access benthic invertebrate prey during migration and wintering periods (Mu & Wilcove, 2020). Any reduction in the area or quality of these tidal flats can therefore directly lower the carrying capacity of the site for migratory birds (Zhang et al., 2023).

In recent years, however, *Spartina alterniflora* has expanded rapidly across the intertidal flats of DMNNR, replacing large areas of open mudflat with dense stands of this invasive grass (Yan et al., 2021). Because unvegetated tidal flats are both a defining ecological feature of the World Heritage property and a critical resource for EAAF migratory birds (Mu & Wilcove, 2020), assessing how *S. alterniflora* control has altered the extent and spatial configuration of intertidal habitats in DMNNR is directly relevant for reserve management and for meeting international biodiversity conservation commitments.

2.3. Remote sensing of *Spartina alterniflora*

Coastal wetlands are typically extensive, tidally influenced and difficult to access, which makes it challenging to monitor them only through field surveys (Davies et al., 2023). Satellite remote sensing can provide repeated, synoptic observations over large areas and has therefore become a core tool for mapping tidal flats, vegetation and invasive species in coastal zones (Zhou et al., 2025). For *Spartina alterniflora* in particular, remote sensing is valuable because the species occupies wide intertidal zones where soft substrates and tidal flooding often prevent comprehensive ground mapping (Min et al., 2025).

Early work on *S. alterniflora* in China mainly used Landsat imagery to reconstruct long-term invasion dynamics. The long historical archive and national coverage of Landsat make it well suited for tracking decadal-scale expansion and partial removal of *S. alterniflora* at sites such as Chongming Island and along the Guangxi coast (Zhang et al., 2020). However, the 30 m spatial resolution of Landsat limits its ability to detect narrow or highly fragmented patches, and small remnant stands after large-scale control are particularly prone to omission (Zhou et al., 2025).

Sentinel-2 provides 10 m spatial resolution in the visible and near-infrared bands, a five-day revisit cycle and four red-edge bands, and its data are freely available. These characteristics improve the spectral separability of different coastal vegetation types and allow much smaller patches of *S. alterniflora* to be resolved compared with Landsat (Liu et al., 2025). A growing number of studies now use Sentinel-2 to map *S. alterniflora* extent and even to estimate above-ground biomass, often by combining multispectral bands and vegetation indices with classification algorithms or regression models (Dong et al., 2024; Zhang et al., 2025; Liu et al., 2025).

In parallel with sensor developments, several specialized spectral indices and phenology-based methods have been proposed for *S. alterniflora*. The *Spartina alterniflora* Index (SAI), derived from Sentinel-2 red and narrow near-infrared bands, uses the characteristic negative index values of *S. alterniflora* during its senescence period to separate it from mudflats and water (Zuo et al., 2025). Multi-site tests across China have shown that SAI-based mapping can reach overall accuracies of about 88–

96% against 3,672 manually labelled samples derived from field surveys and very high-resolution imagery at six representative coastal sites in China (Zuo et al., 2025).

2.4. Methods for mapping *Spartina alterniflora*: Random Forest and SAI

Machine learning-based classification has become the main approach for mapping *Spartina alterniflora* from multispectral imagery at regional and national scales (Zhang et al., 2020; Yan et al., 2021). Among the available algorithms, Random Forest (RF) is one of the most widely used for coastal wetland classification and *S. alterniflora* mapping (Chen et al., 2025). RF is an ensemble method that builds many decision trees on bootstrap samples of the training data and random subsets of predictor variables, and then combines their outputs through majority voting to produce the final class label (Breiman, 2001). In practice, each tree learns a slightly different decision rule from a different subset of pixels and features, and the forest prediction for a new pixel is given by the class that receives the most votes across all trees. This design reduces overfitting compared with a single decision tree, and allows RF to handle high-dimensional input spaces with correlated bands and indices, such as Sentinel-2 multispectral data and derived spectral indices (Belgiu & Drăguţ, 2016). Numerous studies have reported high overall accuracy when RF is applied to classify *S. alterniflora* using Landsat or Sentinel-2 data (Zhang et al., 2020; Dong et al., 2024; Liu et al., 2025).

Despite these advantages, RF has a key limitation: it depends on large, accurately labelled training datasets (Belgiu & Drăguţ, 2016). In intertidal environments, obtaining such datasets is difficult because physical access is restricted by tides, safety concerns and the soft sediment, while the spatial extent of *S. alterniflora* can be very large (Zhou et al., 2025). After large-scale eradication, remaining patches are often harder to collect representative samples that capture the full spectral variability of residual stands. As a result, applying RF for post-eradication mapping may become impractical if reliable training data cannot be gathered for each target year.

To address the dependence on training samples, Zuo et al. (2025) proposed the *Spartina alterniflora* Index (SAI), a simple index constructed from Sentinel-2 red (Band 4) and narrow near-infrared (Band 8A) reflectance, formulated as

$$\mathrm{SAI} = \frac{B_4 - B_{8A}}{B_{8A}} \tag{1}$$

SAI takes advantage of the distinct spectral behavior of *S. alterniflora* during senescence: the species typically exhibits strongly negative SAI values, while surrounding mudflats and water show higher or positive values (Zuo et al., 2025). By defining an appropriate threshold range for SAI, *S. alterniflora* can be extracted across multiple sites without local training samples.

In this thesis, RF and SAI are combined in a complementary way. First, RF is applied to the 2022 Sentinel-2 image to produce a supervised baseline map of *S. alterniflora* and to provide an independent benchmark for assessing the reliability of SAI-based extraction in the same year. Second, SAI thresholds derived from the 2022 sample data are applied unchanged to both the 2022 and 2025 images. This allows *S. alterniflora* to be mapped in 2025 without new training samples, which is essential in a post-eradication scenario where very few patches remain and are difficult to sample.

2.5. Conceptual framework

Based on the considerations above, this study develops a simple and transparent analytical framework for the intertidal zone of DMNNR. In the first step, Sentinel-2 images from 2022 and 2025 are used to produce two *S. alterniflora* maps. For 2022, Random Forest classification is applied, using multispectral bands and spectral indices to build a supervised baseline map. At the same time, suitable SAI thresholds for the study area are determined from the 2022 data. In the second step, the *S. alterniflora* maps derived from RF and SAI in 2022 are compared, so that the supervised classification can be used to evaluate the reliability of the SAI thresholds. On this basis, the same SAI thresholds are applied to the 2025 image, enabling sample-free extraction of *S. alterniflora* in 2025 under conditions where few patches remain and training samples are difficult to obtain. In the third step, the 2022 and 2025 maps are overlaid and summarized to calculate net area change and clearance rate of *S. alterniflora*. Cleared patches, persistent patches and newly established patches are distinguished, and Global Moran's I and kernel density estimation are used to analyze whether the remnant patches show significant spatial clustering and where the main hotspots are located.

3. Methodology

3.1. Study area

The Dafeng Milu National Nature Reserve (DMNNR) (32°56′N–33°36′N, 120°42′E–120°51′E) is located along the Yellow Sea coast in Dafeng District, Yancheng City, Jiangsu Province, eastern China. It forms the southern part of the Yancheng Yellow Sea coastal wetland complex and is an important component of the UNESCO World Natural Heritage site “Migratory Bird Sanctuaries along the Coast of the Yellow Sea-Bohai Gulf of China (Phase I)” (UNESCO, 2019). The reserve covers an area of approximately 78,000 hectares. Its landscape is dominated by typical coastal wetlands, such as intertidal mudflats, salt marshes, reed wetlands, wet grasslands, woodlands, and some artificial wetlands (Yan et al., 2022).

In this study, the selected study area focuses on the intertidal zone located seaward of the eastern seawall of DMNNR (**Fig. 2**). The boundary of the study area was defined in two steps. First, a polygon covering the intertidal zone was manually delineated using remote sensing imagery. The seawall was used as the landward boundary, while the seaward boundary was slightly extended beyond the eastern edge of DMNNR to ensure full coverage of exposed mudflats. The seawall location was identified based on the S2Coast-2023 dataset (Duan et al., 2026), which provides a 10 m resolution global coastline derived from annual cloud-free Sentinel-2 composites, as well as visual interpretation of high-resolution Google Earth imagery. Second, the polygon was clipped using the official boundary of DMNNR to ensure that the final study area was strictly confined within the reserve. This approach ensured that the analysis covered the entire intertidal zone between the seawall and the seaward boundary of the reserve, while excluding reclaimed land, aquaculture ponds, and terrestrial vegetation on the landward side.

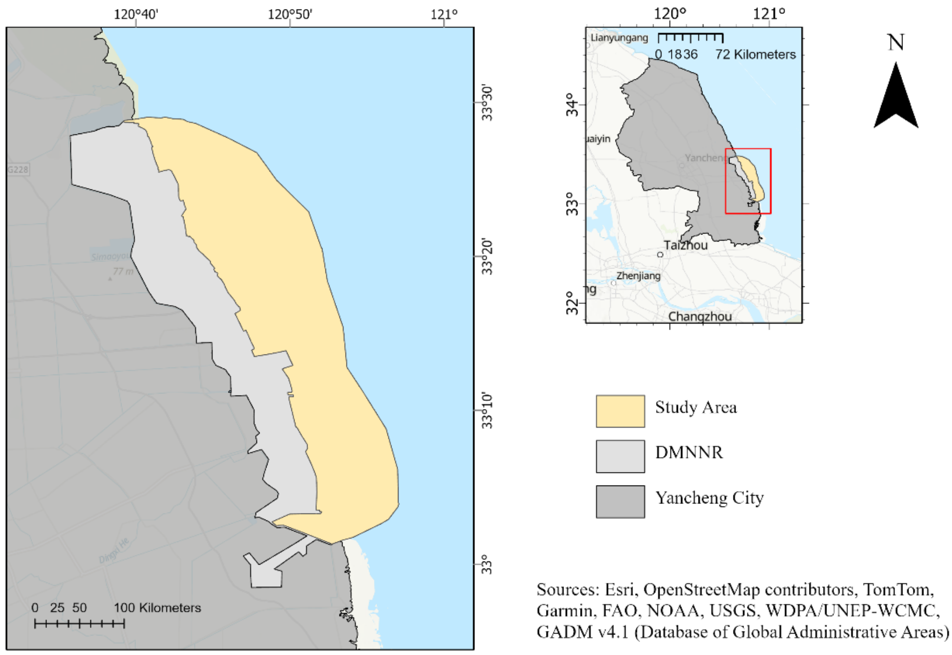

Fig. 2. Study area (yellow) within Dafeng Milu National Nature Reserve (light grey) and Yancheng City boundary (dark grey). The seaward extent was extended beyond the reserve's eastern boundary to include exposed intertidal flats and Seawall location derived from S2Coast-2023(Duan et al., 2026) and Google Earth imagery

From an ecological perspective, this exclusion is reasonable because *Spartina alterniflora* is a low-elevation salt marsh species, typically distributed between mean sea level and mean high tide, and does not establish stable populations on terrestrial habitats landward of the seawall (Kim et al., 2023). In recent years, large-scale removal efforts have been implemented under national control programs. The combination of extensive invasion, intensive recent removal, and the area's importance as a habitat for migratory waterbirds makes DMNNR a representative and meaningful site for evaluating the effectiveness of *Spartina alterniflora* management at the scale of a single protected area.

At the same time, field surveys in the intertidal zone are constrained by tidal dynamics and soft sediment conditions, making it difficult to collect sufficient and evenly distributed training and validation samples for multiple time periods. This limitation highlights the importance of satellite remote sensing as the primary data source. Overall, DMNNR offers a relatively representative intertidal system, making it well suited for testing the proposed framework for evaluating *Spartina alterniflora* management effectiveness using Sentinel-2 imagery.

3.2. Data

Five datasets (**Table 1**) were used in this study to assess the effectiveness of *Spartina alterniflora* control in the intertidal zone of Dafeng Milu National Nature Reserve (DMNNR) between 2022 and 2025. These include Sentinel-2 Level-2A multispectral imagery, the official DMNNR boundary, the S2Coast-2023 coastline dataset, the CM-SSM 2020 national Spartina map, and Google Earth high-resolution imagery.

Table 1. Datasets used in the study.

Dataset	Source	Resolution	Time
Sentinel-2 L2A	ESA/GEE	10-60 m	2022-12-14, 2025-12-18
DMNNR Boundary	WDPA	Vector	2026
CM-SSM 2020	Zhou et al. (2025)	<1 m	2020
S2Coast-2023	Duan et al. (2026)	10 m	2023
Google Earth Imagery	Google	<1 m	2020-2025

3.2.1. Sentinel-2 imagery

Sentinel-2 Multispectral Imagery. Sentinel-2 Level-2A (L2A) surface reflectance imagery was obtained from the Google Earth Engine (GEE) platform (COPERNICUS/S2_SR_HARMONIZED). Two acquisition dates were selected: 2022-12-14 and 2025-12-18, both falling within the senescence period of *S. alterniflora*, during which the spectral contrast between *S. alterniflora* and co-occurring coastal vegetation is maximized (Ouyang et al., 2013).

The reason why this study selected two discrete time points (the baseline condition before management in December 2022 and the post-management result in December 2025), rather than using continuous spatiotemporal imagery, is mainly based on two considerations. First, during the management period (2023–2024), the intertidal zone exhibited a highly fragmented land–water mosaic pattern. Removed patches, waterlogged areas formed by enclosure flooding, and residual stems created a large number of mixed pixels at the 10 m spatial resolution of Sentinel-2. Under these conditions, spectral-based methods have difficulty reliably distinguishing between treated Spartina alterniflora, shallow water, and exposed mudflats, resulting in considerable classification uncertainty. Second, compared with attempting to reconstruct the year-by-year dynamic changes during the management process, the Before–After Control Impact (BACI) design provides a more robust and interpretable assessment of management effectiveness by directly comparing the spatial extent and distribution patterns of *S. alterniflora* before and after management (Seger et al., 2021).

Images were first filtered by a cloud cover threshold of less than 20%, after which candidate scenes were visually inspected to confirm low-tide conditions, ensuring that the intertidal vegetation was fully exposed above the waterline and minimizing the influence of tidal inundation on spectral signatures. The selected images were then mosaicked across tiles to ensure full spatial coverage of the study area. The spectral bands used in this study are summarized in **Table 2**. All imagery was processed on the GEE platform, where multi-spectral bands were automatically resampled to a consistent 10-meter resolution prior to analysis.

Table 2. Sentinel-2 spectral bands used in this study.

Band	Name	Wavelength(nm)	Resolution(m)	Use in this study
B2	Blue	490	10	Classification
B3	Green	560	10	MNDWI, Classification
B4	Red	665	10	SAI, NDVI, Classification
B5	Red Edge 1	705	20	NDRE, CIre, Classification
B6	Red Edge 2	740	20	Classification
B7	Red Edge 3	783	20	CIre, Classification
B8	NIR	842	10	NDVI, NDRE, Classification
B8A	Narrow NIR	865	20	SAI, Classification
B11	SWIR 1	1610	20	MNDWI, Classification
B12	SWIR2	2190	20	Classification

3.2.2. S2Coast-2023 coastline dataset

The S2Coast-2023 global coastline dataset (**Fig. 3**) was used to assist in delineating the landward boundary of the intertidal study area (Duan et al., 2026). S2Coast-2023 is the first global coastline product produced at 10 m resolution from Sentinel-2 imagery, and is derived from annual cloud-free composites using a knowledge-based extraction framework implemented on Google Earth Engine (Duan et al., 2026). The dataset detects a standardized High Water Line indicator from a land–water binary classification and provides coastline vectors in ESRI Shapefile format at 10 m spatial resolution (Duan et al., 2026).

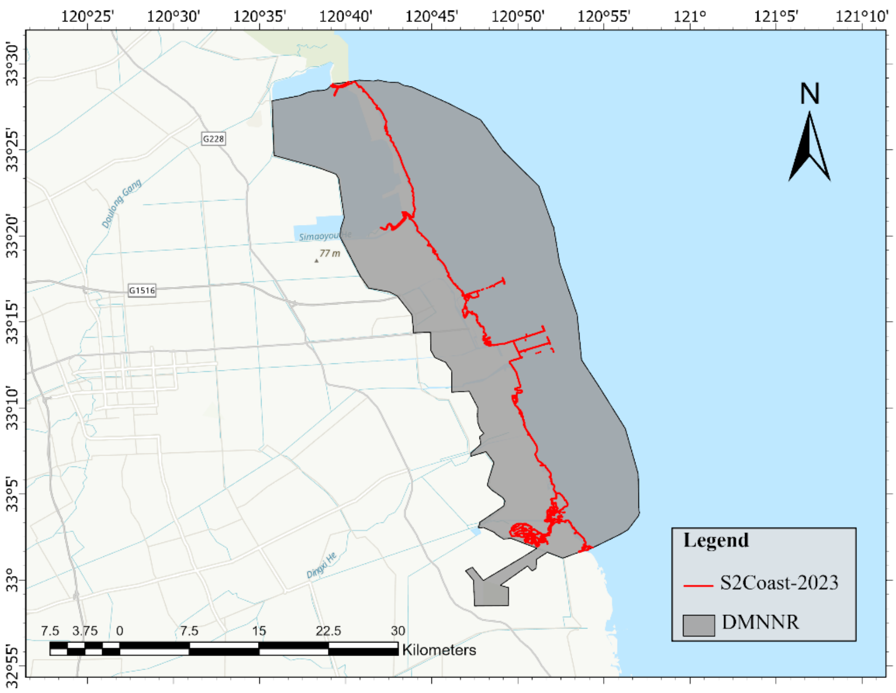

Sources: Esri, OpenStreetMap contributors, TomTom, Garmin, FAO, NOAA, USGS, WDPA/UNEP-WCMC, S2Coast-2023 (Duan et al., 2026)

Fig. 3. The S2Coast-2023 global coastline in DMNNR. The grey polygon represents the reserve boundary, and the red line denotes the S2Coast-2023 coastline, which was used to define the landward edge of the intertidal study area confined within DMNNR.

In this study, the S2Coast-2023 coastline was used as a reference for locating the eastern seawall and the land–sea boundary in the vicinity of DMNNR. Together with visual interpretation of high-resolution Google Earth imagery, it guided the manual digitization of the initial intertidal polygon, which was later clipped to the official DMNNR boundary (see Section 3.1). Using S2Coast-2023 provides a consistent and high-resolution representation of the coastline that is well aligned with Sentinel-2 imagery and reduces potential errors in defining the landward limit of the intertidal zone.

3.2.3. Ancillary data

Several ancillary datasets were used to support the interpretation, mapping and validation of *S. alterniflora*:

DMNNR Boundary. The official boundary of Dafeng Milu National Nature Reserve was obtained from the World Database on Protected Areas (WDPA), maintained by the UN Environment Program World Conservation Monitoring Centre (UNEP-WCMC). The dataset was downloaded from Protected Planet (WDPA profile: https://www.protectedplanet.net/900674). The boundary polygon was used to clip the study area to ensure that all analyses were spatially constrained within the reserve.

Google Earth High-Resolution Imagery. High-resolution imagery available through Google Earth Pro was used to support visual interpretation during sample collection and to verify the spatial boundary of the study area (https://earth.google.com/web/).

CM-SSM 2020 (**Fig. 4**). The China Mangrove and Saltmarsh Map 2020 (CM-SSM 2020), produced by Zhou et al. (2025), provides national-scale sub-meter mapping of *S. alterniflora* distribution in mainland China for the year 2020. The dataset was obtained from Zenodo (https://doi.org/10.5281/zenodo.16296823). This dataset was used as a spatial reference during the collection of training and validation samples, providing prior knowledge of probable *S. alterniflora* locations to guide visual interpretation of Sentinel-2 imagery.

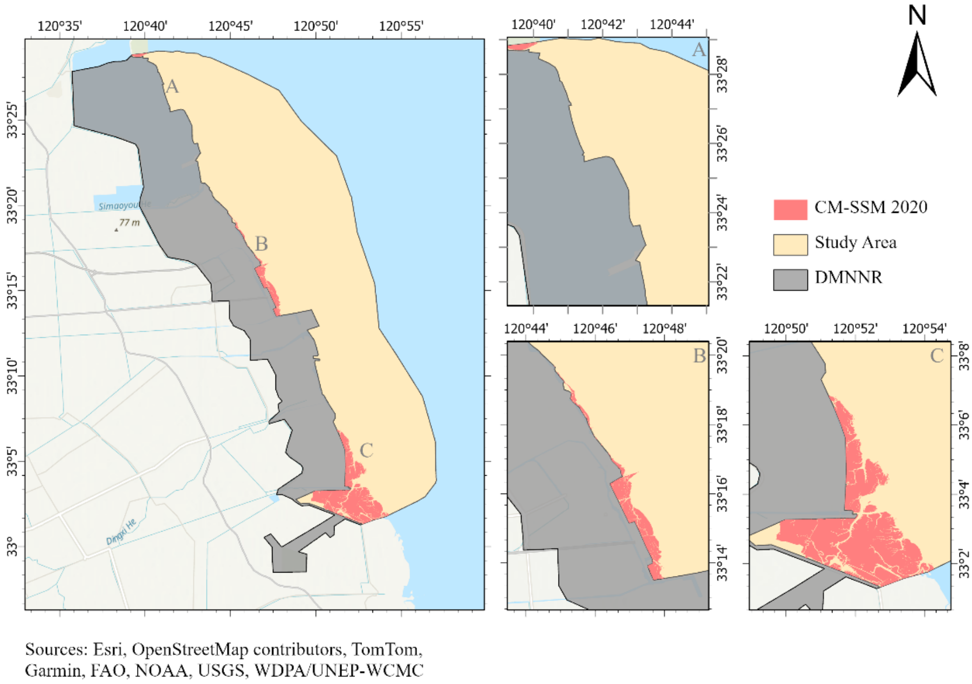

Fig. 4. CM-SSM 2020 *Spartina alterniflora* distribution within the intertidal study area of DMNNR. Panels A–C show enlarged views of the northern, central and southern sections of the study area.

3.3. Method

The overall methodological framework of this study is illustrated in **Fig. 5**.

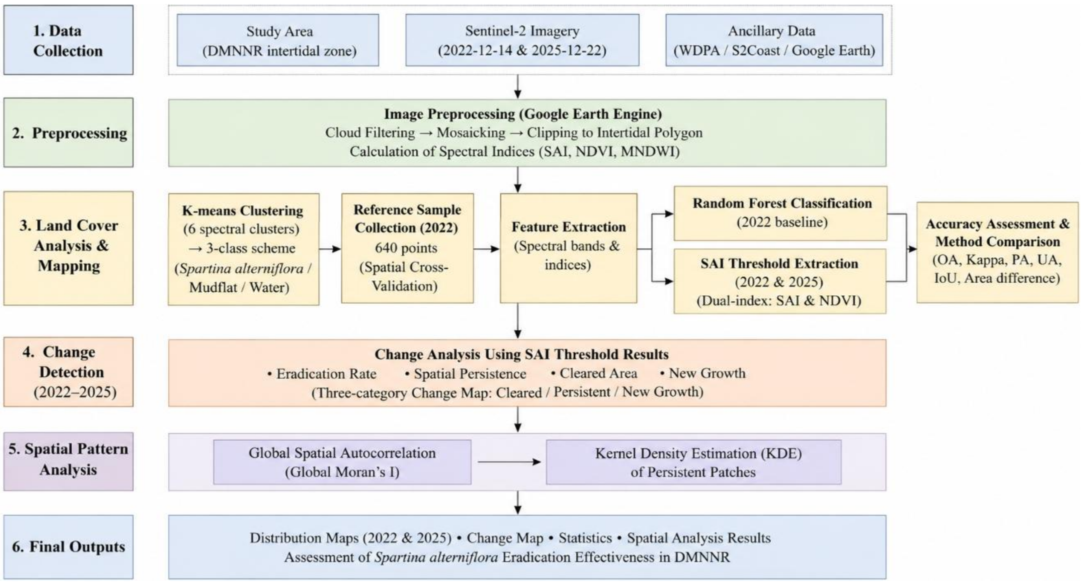

Fig. 5. Workflow of the methodological framework used in this study, showing data collection, image preprocessing, land cover analysis, change detection, spatial pattern analysis, and final assessment of *S. alterniflora* eradication effectiveness in the DMNNR intertidal zone.

3.3.1. Land Cover Composition Analysis

An unsupervised K-means clustering analysis was first conducted in the intertidal study area to assess the composition of land cover types. This step aims to verify whether vegetation types other than *S. alterniflora* exist in the study area such as Phragmites australis, which is commonly found in temperate coastal wetlands in China. This provides empirical support for the design of the subsequent classification scheme.

The feature set used for clustering consists of ten Sentinel-2 spectral bands (B2, B3, B4, B5, B6, B7, B8, B8A, B11, B12) and five spectral indices (SAI, NDVI, MNDWI, NDRE, CIre).

In addition to SAI introduced previously, the Modified Normalized Difference Water Index (MNDWI) and the Normalized Difference Vegetation Index (NDVI) were also included to distinguish water bodies and vegetation, respectively. Two red-edge indices (NDRE, CIre) were further incorporated to maximize spectral separability among different saltmarsh vegetation types.

$$\mathrm{NDVI} = \frac{B8 - B4}{B8 + B4} \tag{2}$$

$$\mathrm{MNDWI} = \frac{B3 - B11}{B3 + B11} \tag{3}$$

$$\mathrm{NDRE} = \frac{B8A - B5}{B8A + B5} \tag{4}$$

$$\mathrm{CI_{re}} = \frac{B7}{B5} - 1 \tag{5}$$

where B3 corresponds to the green band (560 nm) and B11 corresponds to the shortwave infrared (SWIR) band (1610 nm), and is effective for enhancing open water features. B8 represents the near-infrared (NIR) band and B4 represents the red band, and is widely used to characterize vegetation presence and condition. B5 (705 nm) corresponds to the red-edge 1 band sensitive to chlorophyll content, and B8A (865 nm) represents the narrow near-infrared band. B7 (783 nm) and B5 (705 nm) are both red-edge bands, and their combination reflects differences in canopy chlorophyll concentration. *S. alterniflora* and other saltmarsh species such as *Phragmites australis* exhibit significant differences in reflectance within this region due to variations in canopy structure, leaf area index, and chlorophyll content, providing better discrimination than broadband indices such as NDVI (Ouyang et al., 2013).

A total of 8,000 pixels were randomly sampled within the study area to train the clustering model (Fig. 6). The clustering algorithm was implemented using the K-Means clusterer (ee.Clusterer.wekaKMeans) on the GEE platform, with the number of clusters set to six (k = 6). Training samples were extracted from the Sentinel-2 image composite using spectral bands (B2, B3, B4, B5, B6, B7, B8, B8A, B11, B12) along with derived indices including SAI, NDVI, MNDWI, NDRE, and CIre as input features. The clusterer was trained on this sample set and subsequently applied to the full study area image (Moussaid et al., 2026). The clustering results were interpreted by analyzing the mean values of these spectral bands and indices for each cluster, combined with visual interpretation of false-color composite imagery and reference datasets.

Fig. 6. Spatial distribution of 8,000 randomly sampled pixels used for K-means clustering in the intertidal study area of DMNNR. Panels A–C show enlarged views of the northern, central and southern sections of the study area.

3.3.2. Sample Collection

A total of 640 reference sample points (**Fig. 7**) were collected for three land-cover classes: *Spartina alterniflora* (n = 240), mudflat (n = 200) and water body (n = 200). The sample size follows commonly used guidelines for thematic map accuracy assessment, which recommend a minimum of about 50 reference samples per class and higher numbers (75–100 or more) for classes of particular importance or with high internal variability (Wulder et al., 2006). *S. alterniflora* is the focal class in this study and exhibits substantial spectral variability across dense monocultures, sparse stands and transitional patches at mudflat margins, whereas mudflat and water are comparatively homogeneous. Consequently, the number of *S. alterniflora* samples was increased to 240, while mudflat and water were allocated 200 samples each.

All samples were collected manually within the Google Earth Engine (GEE) platform by expert visual interpretation of multiple layers: (i) the Sentinel-2 Level-2A false colour composite (bands B8A/B4/B3) for 14 December 2022, (ii) the CM-SSM 2020 *S. alterniflora* distribution map, and (iii) high-resolution optical imagery from Google Earth. High-resolution imagery and existing land cover products were recognized as prior information to guide the delineation of reliable reference samples.

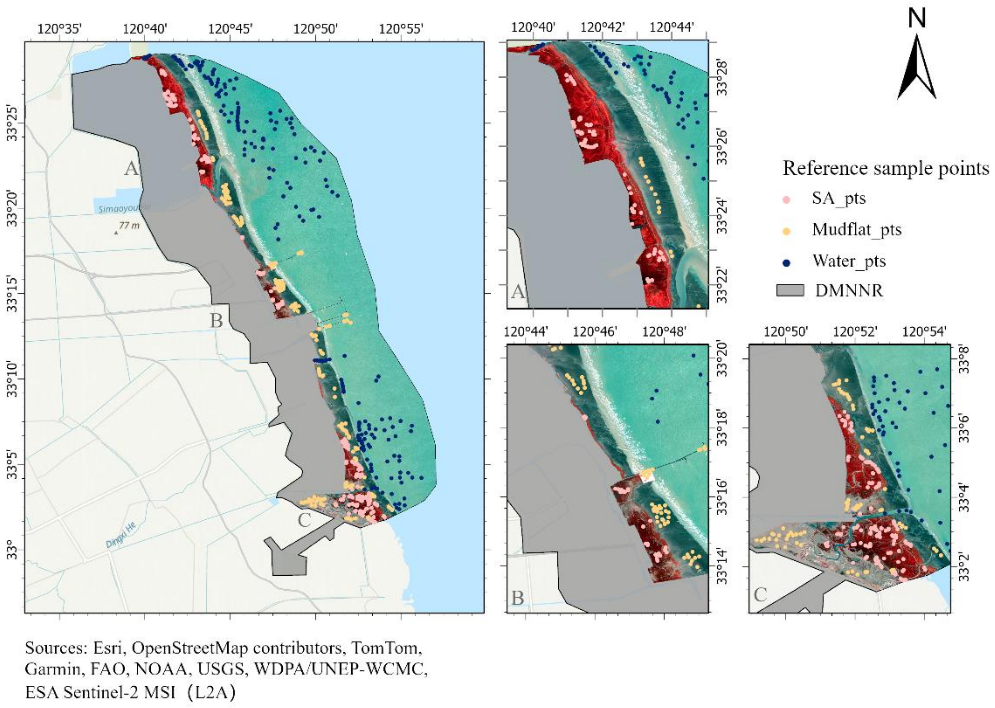

Fig. 7. Reference sample points for *Spartina alterniflora*, mudflat and water body collected from the 14 December 2022 Sentinel-2 image within the intertidal study area of Dafeng Milu National Nature Reserve (DMNNR). Panels A–C show enlarged views of the northern, central and southern sections of the study area.

For *S. alterniflora*, sample points were preferentially placed within patches that were consistently identified as *S. alterniflora* in both the CM-SSM 2020 map and the high-resolution Google Earth imagery, and that exhibited the expected spectral appearance in the Sentinel-2 false colour composite. Mudflat samples were selected from unvegetated intertidal areas with varying moisture conditions (dry and moist mudflat) and no visible vegetation cover in Google Earth. Water samples were located in tidal channels and nearshore waters that were consistently classified as water across all reference layers.

Three MultiPoint geometry layers were digitized in GEE, one for each class, and exported as assets for use in both the SAI threshold determination and the Random Forest training workflow. Class labels were assigned programmatically during the sampling and classification steps based on the layer of origin rather than being stored as attributes in the original MultiPoint assets.

It should be noted that all reference samples are derived from image-based expert interpretation rather than from independent field surveys or airborne data. Consequently, they should be regarded as high-quality reference labels rather than absolute ground truth, and residual labelling errors may partially influence both the Random Forest model and the SAI threshold statistics. This limitation is explicitly considered in the interpretation of the eradication results.

3.3.3. Random Forest Classification

Random Forest (RF) classification was applied to the 2022 Sentinel-2 imagery to generate a supervised three-class land cover map of the intertidal study area, which was used as the baseline map for subsequent comparison with the 2025 extraction. The classifier was implemented using the smileRandomForest algorithm in Google Earth Engine (GEE). The input feature stack comprised ten Sentinel-2 spectral bands (B2, B3, B4, B5, B6, B7, B8, B8A, B11, and B12) together with two spectral indices, NDVI and MNDWI, resulting in 12 predictor variables in total. The target classes were *S. alterniflora*, mudflat, and water, as defined by the reference samples described in Section 3.3.1.

To reduce the influence of spatial autocorrelation on model evaluation, a simple spatial block cross-validation strategy was adopted instead of randomly splitting the reference samples, following recent recommendations for spatially structured ecological and remote sensing data (Roberts et al., 2017; Stock, 2025). All 640 reference points were first assigned planar coordinates in GEE, and the x-coordinate was used to divide the study area into western and eastern spatial blocks. Samples located in the western block were used for model training, whereas those in the eastern block were reserved for validation. This design ensured a clear spatial separation between training and validation data while maintaining representation of all three land cover classes in both blocks.

Rather than relying on default settings, the RF hyperparameters were tuned using a small grid-search procedure based on the spatially independent validation block (Hengl et al., 2018). Two key parameters were first explored: the number of trees (numberOfTrees) and the minimum leaf population (minLeafPopulation). The number of trees was tested across 100, 200, 300, and 500, while the minimum leaf population was tested across 1, 3, 5, and 10. During this step, the bagging fraction (bagFraction) was fixed at 0.7 to isolate the effects of the other two parameters. Because the tested configurations produced only minor differences in validation performance, the RF model was considered relatively insensitive to these parameter settings for the present dataset. A configuration of numberOfTrees = 200 and minLeafPopulation = 3 was therefore selected as a practical compromise between model stability and computational efficiency.

In a second tuning step, the bagging fraction was varied between 0.6, 0.7, and 0.8 while keeping numberOfTrees = 200 and minLeafPopulation = 3 fixed. As only negligible differences were observed among these values, bagFraction = 0.7 was retained for the final model, as it represents a conventional intermediate setting that provides a balance between ensemble diversity and model stability.

The final RF model was therefore trained using numberOfTrees = 200, minLeafPopulation = 3, and bagFraction = 0.7, and then applied to the full 2022 feature stack within the intertidal polygon to produce the baseline land cover classification map.

Accuracy was assessed using the validation set by constructing a confusion matrix and computing the following metrics, which were chosen because they are directly provided by the GEE errorMatrix function and commonly used in remote sensing (Congalton, 1991; Foody, 2002). Overall accuracy (OA) measures the proportion of correctly classified samples across all classes:

$$\mathrm{OA} = \frac{\sum_{i=1}^{k} n_{ii}}{N} \tag{6}$$

where $\mathrm{n_{ii}}$ is the number of correctly classified samples for class i, k is the number of classes, and *N* is the total number of validation samples. The Kappa coefficient ($\widehat{\mathrm{K}}$) accounts for agreement occurring by chance:

$$\widehat{K} = \frac{N\sum_{i=1}^{k} n_{ii} - \sum_{i=1}^{k}(n_{i+} \cdot n_{+i})}{N^2 - \sum_{i=1}^{k}(n_{i+} \cdot n_{+i})} \tag{7}$$

where $\mathrm{n_{i+}}$ and $\mathrm{n_{+i}}$ denote the row and column marginal totals for class i. Producer's accuracy (PA) and user's accuracy (UA) were calculated for each class as:

$$\mathrm{PA_i} = \frac{n_{ii}}{n_{i+}}, \ \mathrm{UA_i} = \frac{n_{ii}}{n_{+i}} \tag{8}$$

PA reflects the probability that a reference sample of a given class is correctly classified (omission error = 1 − PA), while UA reflects the probability that a classified pixel actually belongs to that class (commission error = 1 − UA) (Congalton, 1991; Foody, 2002).

3.3.4. SAI Threshold Extraction

The SAI threshold method was adopted as the primary approach for *S. alterniflora* mapping. Requiring no training samples, it can be applied consistently across different years, making it particularly suitable for the 2025 post-eradication scenario where the scarcity of remnant *S. alterniflora* patches precludes reliable sample collection and hard to be classified by RF.

The SAI threshold range for *S. alterniflora* was determined statistically from the 2022 sample dataset. SAI values were extracted at all 640 sample points and class-wise box plots were constructed for the three land cover classes. Following the approach of Zuo et al. (2025), the threshold was determined using the standard 1.5 × IQR (interquartile range) method. For each class, the lower and upper fences were computed as Q1 − 1.5 × IQR and Q3 + 1.5 × IQR respectively, where Q1 and Q3 denote the first and third quartiles. Sample values falling beyond these fences are classified as outliers and excluded from the whisker range.

An additional NDVI constraint was applied alongside the SAI threshold to exclude pixels whose SAI values may occasionally fall within the *S. alterniflora* range due to high surface moisture content. The NDVI bounds were determined by the same 1.5 × IQR whisker procedure applied to the *S. alterniflora* NDVI distribution in the 2022 sample dataset.

To evaluate the reliability of the SAI threshold method, its 2022 extraction result was compared against the RF classification result using two metrics: (1) the area difference expressed as a percentage of the RF-derived area, and (2) the Intersection over Union (IoU), defined as the ratio of the spatial intersection to the spatial union of the two binary maps. A spatial agreement map was also produced to distinguish pixels classified as *S. alterniflora* by both methods (agreement), by RF only, and by SAI only. The same threshold values and dual-index constraints were applied without modification to the 2025 imagery, ensuring methodological consistency between the two time points.

3.3.5. Spectral Distribution Analysis

To further support the threshold determination and to provide spectral-level evidence of *S. alterniflora* change between the two time points, SAI and NDVI frequency histograms were generated for both the 2022 and 2025 imagery across the full study area in GEE. For SAI, a focused histogram restricted to SAI < 0 to highlight the distribution of vegetated pixels was produced. For NDVI, a histogram restricted to NDVI > 0 was produced for each year to emphasize the vegetation signal.

The histograms serve two purposes. First, they provide a visual basis for confirming that the adopted SAI threshold range corresponds to a distinct spectral peak in the 2022 distribution, rather than being arbitrarily imposed. Second, comparison of the 2022 and 2025 histograms provides direct spectral evidence of *S. alterniflora* change: a reduction or disappearance of the negative SAI peak between years would indicate large-scale eradication, independent of the quantitative area estimates.

3.3.6. Change Analysis

To assess the effectiveness of the *S. alterniflora* eradication campaign, a quantitative change analysis was conducted by comparing the SAI-based extraction results between 2022 and 2025. Three metrics were calculated:

Eradication rate. The proportion of the 2022 *S. alterniflora* area that was no longer detected in 2025, calculated as

$$\frac{A_{2022}-A_{2025}}{A_{2022}} \times 100\% \tag{9}$$

where A_{2022} and A_{2025} denote the *S. alterniflora* area extracted by the SAI method in 2022 and 2025, respectively.

Spatial persistence. Pixels classified as *S. alterniflora* in both 2022 and 2025 were identified as persistent patches, representing areas where eradication was incomplete. The spatial distribution of persistent patches was mapped to identify locations of remaining *S. alterniflora* within the reserve.

Cleared area. Pixels present in the 2022 extraction but absent in 2025 were identified as cleared areas, representing locations where eradication was successful.
New growth. Pixels absent in the 2022 extraction but present in 2025 were identified as potential new growth areas.

The spatial change map was produced by combining the two binary extraction results into a three-category map: cleared (2022 only), persistent (both years), new growth (2025 only). All change metrics were calculated on the GEE platform using pixel-wise logical operations on the clipped binary images.

3.3.7. Spatial Pattern Analysis of Persistent Patches

The three-class change map (cleared, persistent, new growth) produced in Google Earth Engine was exported as a GeoTIFF and clipped to the intertidal study area in ArcGIS Pro 2.7.

Persistent pixels were isolated from the change raster using an attribute-based mask, and converted to polygons using the Raster to Polygon tool (Conversion toolbox) in ArcGIS Pro. The resulting polygon layer represents the spatial extent of all persistent *S. alterniflora* patches in 2025 within the study area.

To obtain one representative location per patch, polygon centroids were generated with the Feature To Point tool (Data Management toolbox), enforcing the “Inside” option so that each point fell within its corresponding polygon. These centroids were used as inputs to the spatial statistics analyses, treating each persistent patch as a single event.

Global spatial autocorrelation of persistent patches was evaluated with the Global Moran's I statistic using the Spatial Autocorrelation (Global Moran's I) tool (Spatial Statistics toolbox) in ArcGIS Pro. Patch identifiers (ID) were used as the input field, effectively assigning equal weight to all patches while testing whether their locations deviate from spatial randomness. A fixed distance band of 2 km and row-standardized spatial weights were adopted to represent neighborhood relationships within the intertidal zone. Statistical significance was assessed using z-scores and p-values under the randomization null hypothesis.

To visualize spatial concentrations of persistent patches, kernel density estimation (KDE) was applied to the patch centroids using the Kernel Density tool (Spatial Analyst toolbox) in ArcGIS Pro. KDE was computed with a search radius of 2 km and an output cell size of 100 m, with no population field specified so that each patch contributed equally to the density surface.

4. Results

4.1. Land Cover Composition

The K-means clustering analysis identified six spectrally distinct land cover classes within the intertidal study area (**Table 3, Fig. 8**). The interpretation of each class was based on the mean SAI, NDVI, and MNDWI values and Google Earth. Class 4 was the only cluster exhibiting spectral characteristics consistent with vegetation, with a mean SAI of −0.626 and mean NDVI of 0.469, well within the range expected for *S. alterniflora* during its senescence period. This class occupied an area of 3,063 ha. Critically, no other cluster displayed a combination of strongly negative SAI and NDVI exceeding 0.2, confirming that no additional salt marsh vegetation was present within the delineated intertidal zone. These results justify the adoption of a simplified three-class scheme (*S. alterniflora*, mudflat, water body) for subsequent Random Forest classification and SAI threshold extraction.

Table 3. K-means clustering results for the intertidal study area (2022-12-14), showing mean spectral index values and interpreted land cover class for each cluster.

Class	Interpretation	Mean SAI	Mean NDVI	Mean MNDWI	Area (ha)
0	Shallow water	0.083	0.027	0.818	2,643
1	Landward flat	−0.202	0.147	−0.220	2,115
2	Seaward flat	−0.068	0.078	0.148	5,584
3	Open water	0.324	−0.045	0.864	25,793
4	*S. alterniflora*	−0.626	0.469	−0.468	3,063
5	Deep water	0.484	-0.082	0.876	8396

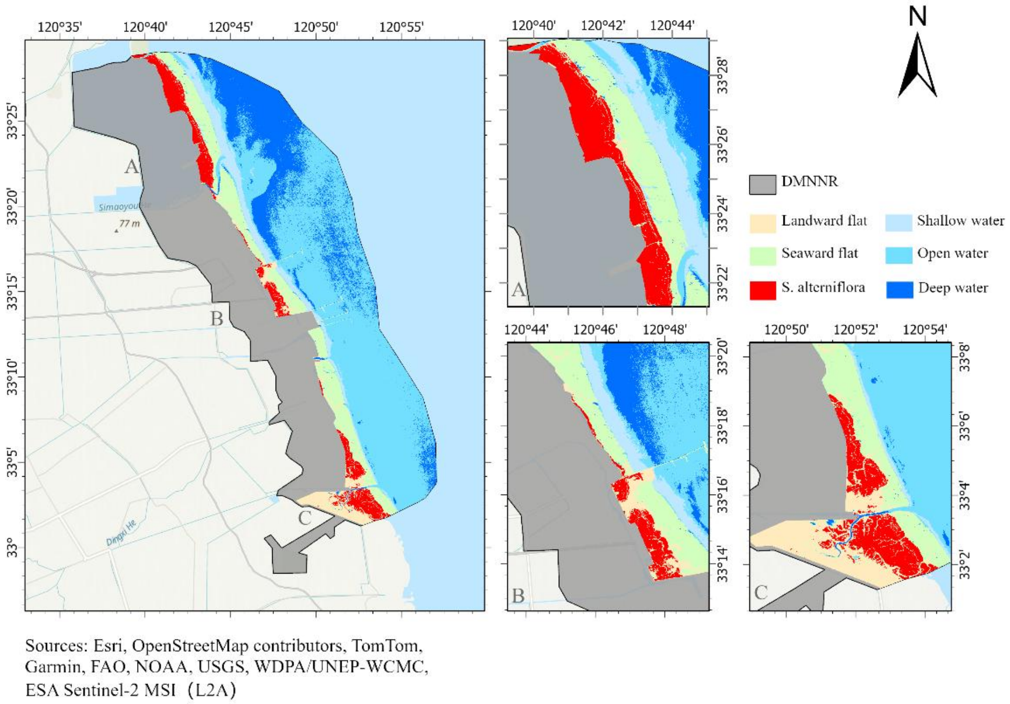

Fig. 8. Unsupervised k-means classification of intertidal land cover (six spectral clusters) used to derive the three-class scheme for subsequent Random Forest modelling.

4.2. SAI Threshold Determination

The SAI and NDVI distributions of the three land cover classes, derived from 640 sample points collected in the 2022 imagery, are summarized in **Table 4** and shown in **Fig. 9.**

Table 4. SAI and NDVI statistical distributions for the three land cover classes based on 640 sample points (2022-12-14).

Class	Index	Min	Q1	Median	Q3	Max	IQR	Outliers
S. alterniflora	SAI	-0.790	-0.691	-0.654	-0.568	-0.388	0.123	0
Mudflat	SAI	-0.490	-0.137	-0.101	-0.066	0.213	0.071	16
Water	SAI	0.032	0.273	0.350	0.429	2.922	0.156	14
S. alterniflora	NDVI	0.275	0.409	0.494	0.536	0.650	0.127	0
Mudflat	NDVI	-0.048	0.072	0.089	0.105	0.251	0.032	18
Water	NDVI	-0.455	-0.069	-0.050	-0.031	0.041	0.039	12

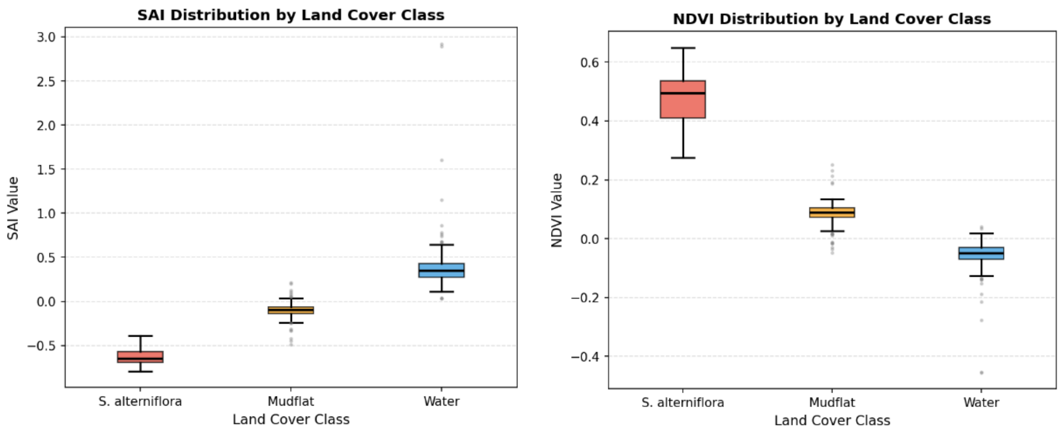

Fig. 9. Boxplots illustrating the distribution of SAI and NDVI values among three classes.

For SAI, the three classes exhibited complete spectral separation with no overlap between whisker ranges. *S. alterniflora* showed the most strongly negative SAI values, ranging from −0.790 to −0.388 (median: −0.654, IQR: 0.123), with zero outliers, indicating a compact spectral distribution. Mudflat occupied a higher SAI range of −0.239 to +0.040 (median: −0.101), and water body ranged from +0.108 to +0.642 (median: +0.350). The gap between the *S. alterniflora* upper whisker (−0.388) and the mudflat lower whisker (−0.239) was 0.149, confirming the clear spectral distinctiveness of *S. alterniflora* within the study area.

For NDVI, separation between classes was equally clear. *S. alterniflora* ranged from 0.275 to 0.650 (median: 0.494), substantially above the mudflat upper whisker of 0.136 and the water body upper whisker of 0.018.

Based on the 1.5 × IQR whisker method following Zuo et al. (2025), the adopted dual-index extraction condition for *S. alterniflora* was:

$$-0.790 \leqslant SAI \leqslant -0.388 \text{ AND } 0.275 \leqslant NDVI \leqslant 0.650$$

The SAI threshold range is broadly consistent with the range reported by Zuo et al. (2025) for YNNR（Yancheng National Nature Reserve, closed to DMNNR） (−0.75 to −0.60), with the wider upper bound (−0.388 vs −0.60) attributable to the inclusion of sparse and transitional *S. alterniflora* patches in the sample dataset, which exhibit less negative SAI values due to lower canopy density.

4.3. RF Classification and SAI Extraction Comparison in 2022

The Random Forest (RF) classifier achieved an overall accuracy (OA) of 94.97% and a Kappa coefficient of 0.924 based on spatial cross-validation (**Table 5**). Producer's accuracy (PA) for *S. alterniflora* was 94.29%, indicating that 94.29% of actual *S. alterniflora* pixels were correctly identified, while user's accuracy (UA) was 92.31%, indicating that 92.31% of pixels classified as *S. alterniflora* were correctly labelled. Misclassification was largely confined to the boundary between *S. alterniflora* and mudflat: eight *S. alterniflora* pixels were incorrectly assigned to mudflat, and eleven mudflat pixels were incorrectly assigned to *S. alterniflora*. Water body was classified with perfect accuracy (PA = UA = 100%). Consistent with these accuracy metrics, the RF classification mapped a total *S. alterniflora* area of 3,010.32 ha in the intertidal zone of DMNNR in December 2022 (**Fig. 10**), showing continuous monospecific belts along the seaward margin of the reserve.

Table 5. Confusion matrix for RF classification (spatial cross-validation).

	S. alterniflora	**Mud**	**Water**
S. alterniflora	132	8	0
Mud	11	118	0
Water	0	0	109

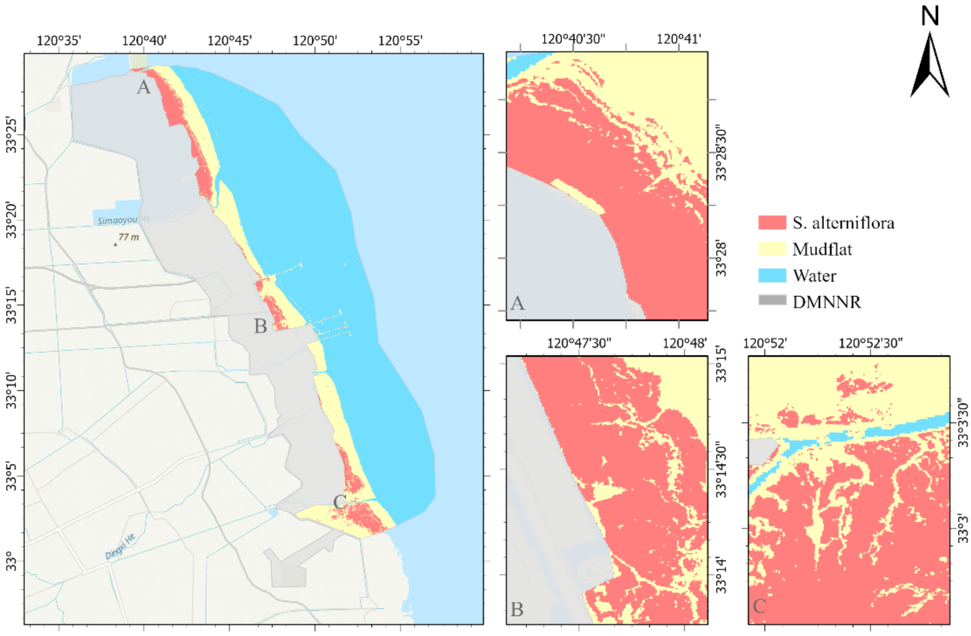

Fig. 10. Random Forest classification of intertidal *Spartina alterniflora*, mudflat, and water in the DMNNR from Sentinel-2 imagery (December 2022), with insets A–C showing detailed patterns along the northern, central, and southern shoreline segments.

Feature importance analysis was not further pursued for the RF model in this study for two main reasons. First, the RF classifier already achieved high and spatially robust accuracy under a spatial block cross-validation design, which is sufficient for its intended role as a baseline land-cover map for subsequent change analysis. Additional feature selection based on importance rankings would therefore have offered limited potential for improving classification performance, while increasing the risk of overfitting or instability. Second, the primary objective of the RF application here is to obtain a reliable and generalizable map of *S. alterniflora*, mudflat, and water, rather than to optimize a minimal subset of predictors or to interpret band-level contributions in detail. For these reasons, all predictor variables were retained in the final RF model, and no additional feature importance-driven variable reduction was implemented.

Applying the dual-index threshold condition to the 2022 imagery yielded a *S. alterniflora* area of 3,147.86 ha, which is 137.55 ha (4.57%) larger than the RF-derived estimate (**Fig. 11**).

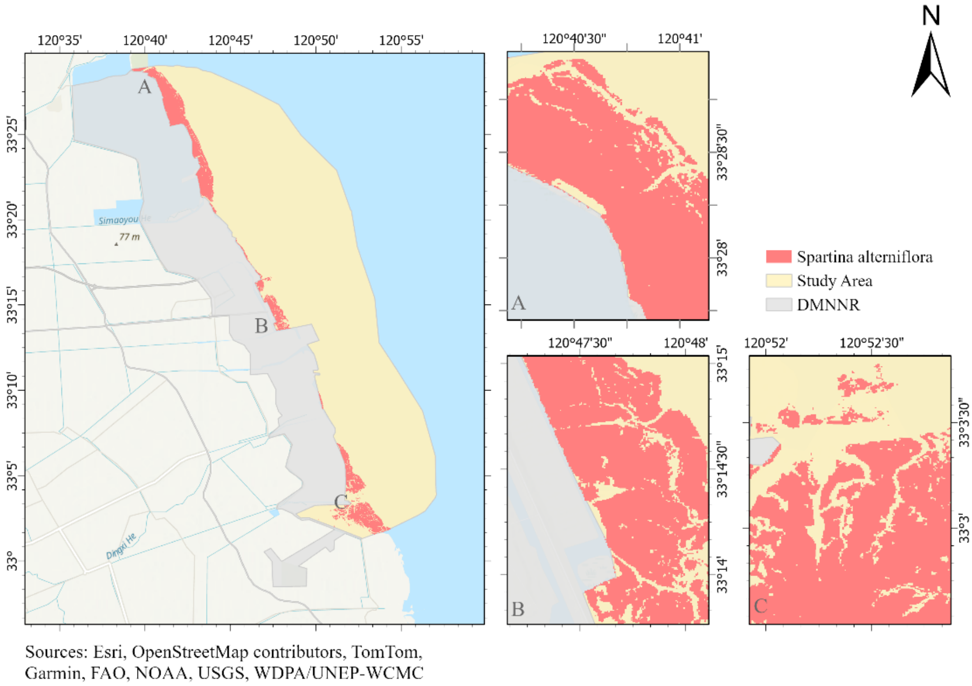

Fig. 11. *Spartina alterniflora* extent in the intertidal zone of the DMNNR in December 2022 derived from the SAI–NDVI dual-index threshold applied to Sentinel-2 imagery, with insets A–C highlighting local patch structure in the same subregions as Fig. 8.

The threshold-based map captures a similar spatial pattern of *S. alterniflora* dominance along the outer tidal flat, but with slightly more extensive coverage at patch edges and in narrow fringing stands. Spatial overlap analysis between the two binary extraction results yielded an IoU of 0.916, indicating that 91.6% of the combined spatial extent was consistently identified by both methods. The spatial agreement map (**Fig. 12**) shows that areas of disagreement are predominantly located at patch margins, where the SAI threshold method tends to map additional, spectrally mixed pixels as *S. alterniflora*. The high IoU and low area difference (4.57%) confirm that the SAI threshold method produces results highly consistent with the supervised RF classification for the 2022 baseline, supporting its application to the 2025 imagery where training samples are unavailable.

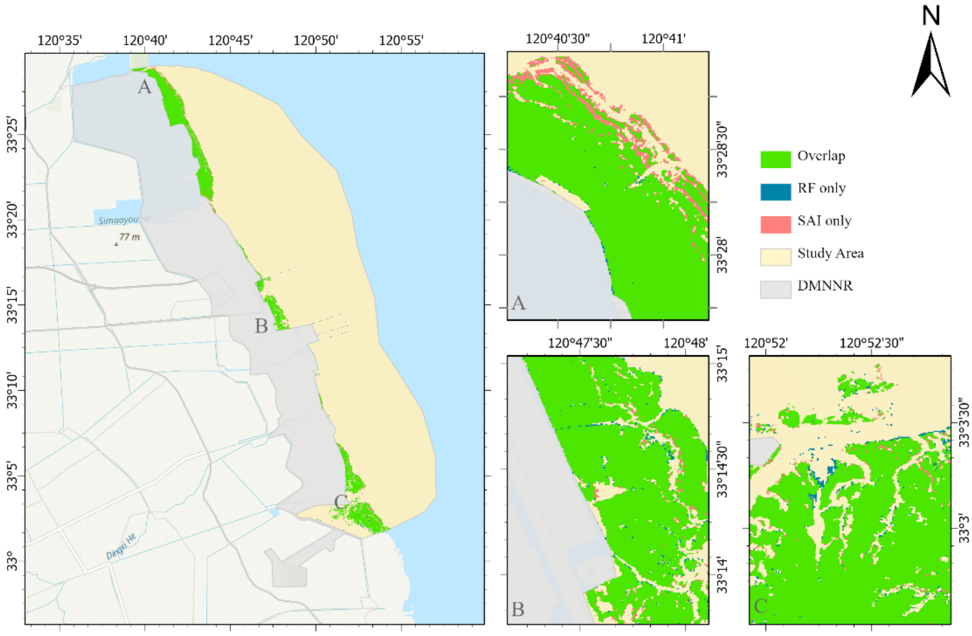

Fig. 12. Spatial agreement between the Random Forest and SAI–NDVI threshold classifications of *Spartina alterniflora* from Sentinel-2 imagery in December 2022, where green indicates overlap, blue indicates RF only, and red indicates SAI only, with insets A–C illustrating discrepancies concentrated at patch margins.

In this study, RF and SAI are not treated as independent alternative classifiers but as two tightly linked components of a single validation framework. RF uses a high-dimensional feature space (multispectral bands plus indices) and spatially independent training–test splits to produce a baseline S. alterniflora map for 2022 with quantified accuracy. The same reference samples are then used to derive site-specific SAI and NDVI thresholds, and the RF baseline provides an independent benchmark against which the SAI extraction can be evaluated using area difference and IoU.

4.4. Spectral Distribution Analysis

The SAI and NDVI histograms for 2022 and 2025 are presented in **Fig. 13**, providing spectral-level evidence of *S. alterniflora* change between the two time points.

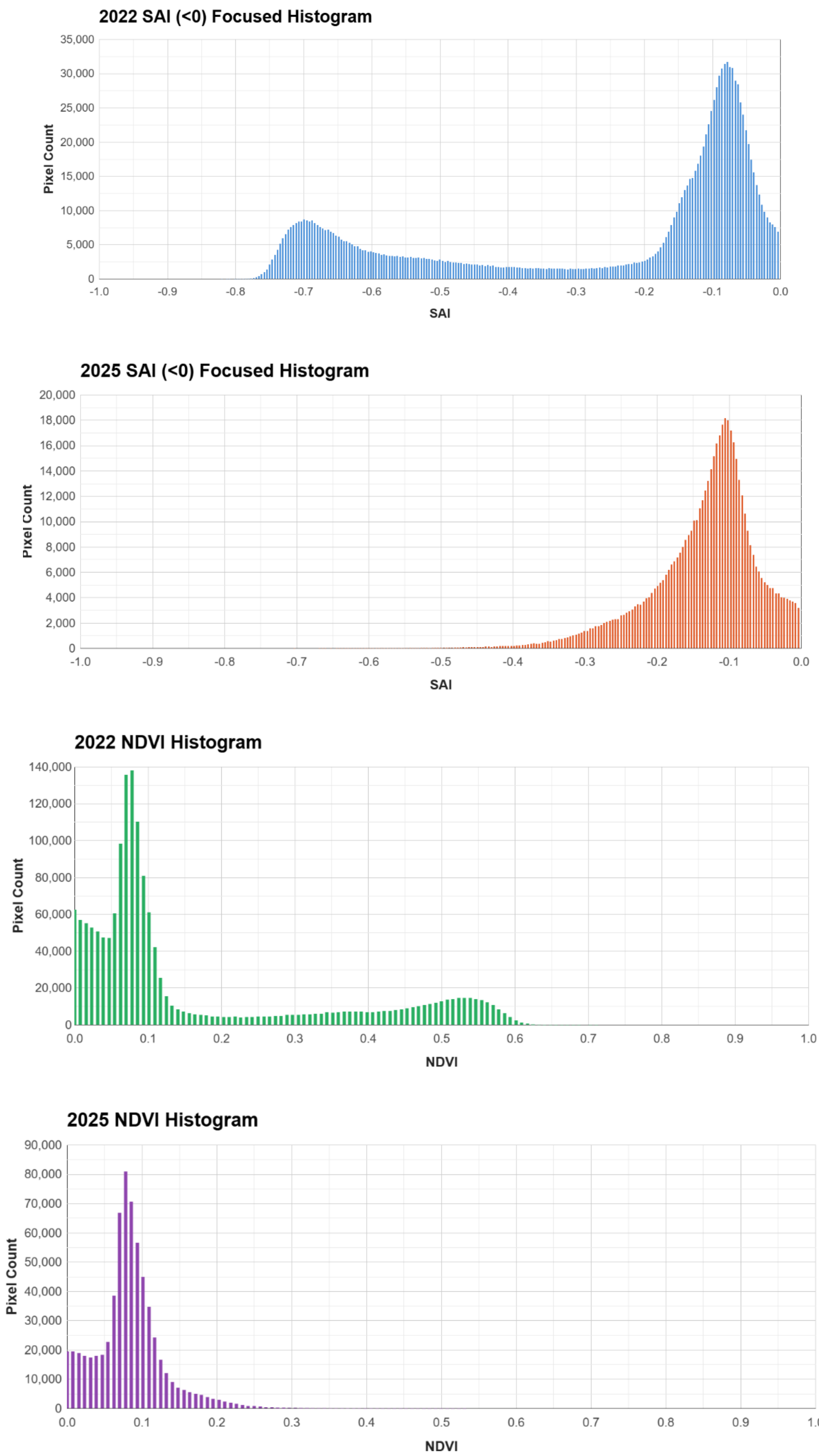

Fig. 13. The SAI (<0) focused and NDVI histograms for 2022 and 2025. The 2022 SAI histogram displays a bimodal distribution with one peak corresponding to *S*.

alterniflora and another representing bare mudflats, while the 2025 SAI histogram presents a unimodal distribution where the *S. alterniflora* peak vanishes. The paired NDVI histograms further verify this change: a prominent secondary peak of S. alterniflora exists in the 2022 dataset and is absent in the 2025 results, jointly demonstrating the near-total removal of *S. alterniflora* in the intertidal zone by 2025.

The 2022 SAI focused histogram (SAI < 0) exhibited a bimodal distribution. A distinct negative peak centered at approximately −0.70 corresponded to the *S. alterniflora* spectral signature and aligned closely with the sample-derived threshold range of [−0.790, −0.388]. A second, larger peak centered at approximately −0.10 was attributed to wet mudflat. A low-frequency transitional zone separated the two peaks, confirming their spectral distinctiveness. In contrast, the 2025 SAI focused histogram showed a unimodal distribution, with only the mudflat peak remaining at approximately −0.10. The *S. alterniflora* peak at −0.70 had entirely disappeared, with pixel counts in the SAI range below −0.45 reduced to near zero. This spectral-level change constitutes independent evidence of large-scale *S. alterniflora* eradication within the study area between 2022 and 2025.

The NDVI histograms corroborated this finding. The 2022 distribution showed a dominant primary peak at approximately 0.08, attributable to mudflat and water body pixels with low vegetation signal, and a distinct secondary peak centered at approximately 0.50–0.55, consistent with the *S. alterniflora* NDVI range identified in the sample statistics (0.275–0.650). By 2025, the secondary vegetation peak had completely disappeared, with pixel counts declining to near zero beyond NDVI = 0.30. The simultaneous disappearance of the *S. alterniflora* spectral signatures in both SAI and NDVI distributions indicated the near-complete eradication of *S. alterniflora* within the DMNNR intertidal zone by December 2025.

4.5. Change Analysis

The SAI-based extraction results for 2022 and 2025 reveal a near-complete eradication of *S. alterniflora* within the intertidal zone of DMNNR over the three-year management period. The total *S. alterniflora* area decreased from 3147.86 ha in December 2022 to 22.84 ha in December 2025, representing an eradication rate of 99.27%. The spatial change map is presented in **Fig. 14**, and the area statistics are summarized in **Table 6**.

Table 6. *S. alterniflora* area change statistics between December 2022 and December 2025 based on SAI threshold extraction.

Category	**Area (ha)**	**% of 2022 extent**
S. alterniflora 2022	3147.86	100%
S. alterniflora 2025	22.84	0.73%
Cleared (2022 only)	3141.92	99.81%
Persistent (both years)	5.95	0.19%
New growth (2025 only)	16.89	0.54%
Eradication rate	99.27%	99.27%

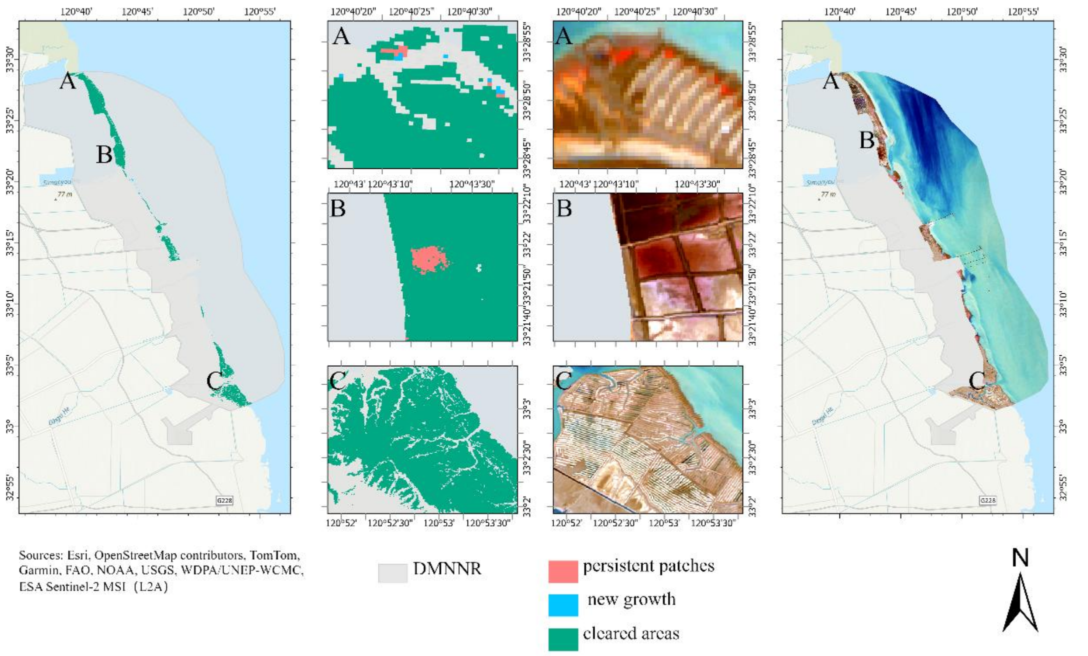

Fig. 14. Spatial distribution of *Spartina alterniflora* change categories in the intertidal zone of the DMNNR between December 2022 and December 2025, derived from SAI-based extraction of Sentinel-2 imagery; green indicates cleared areas (present in 2022, absent in 2025), red indicates persistent patches (present in both years), blue indicates new growth (absent in 2022, present in 2025), and insets A–C show zoomed examples of persistent and new growth patches against false-colour Sentinel-2 composites.

Of the 3147.86 ha present in 2022, 3141.92 ha (99.81%) was classified as cleared by December 2025, indicating that eradication was effective across virtually the entire former *S. alterniflora* extent. Persistent patches accounted for only 5.95 ha (0.19%) of the 2022 extent, suggesting that complete eradication was achieved across almost all of the reserve. New growth pixels, defined as areas absent in 2022 but present in 2025, totaled 16.89 ha (0.54%), representing newly occurred patches. The combined remnant area in 2025 (persistent + new growth = 22.84 ha) constitutes less than 1% of the 2022 baseline extent.

These results are consistent with the spectral evidence presented before, where the near-complete disappearance of the *S. alterniflora* SAI peak (−0.70) and NDVI secondary peak (0.50–0.55) in the 2025 histograms. The spatial distribution of persistent and new growth patches will be examined in detail in the spatial pattern analysis.

4.6. Spatial Pattern Analysis of Persistent Patches

Global Moran's I revealed a strongly clustered distribution of persistent *S. alterniflora* patches in 2025. The index was 0.95, with an expected value of −0.01 under spatial randomness, and a z-score of 23.66 ($p < 0.001$), clearly rejecting the null hypothesis that persistent patches are randomly distributed within the intertidal zone (**Fig. 15**).

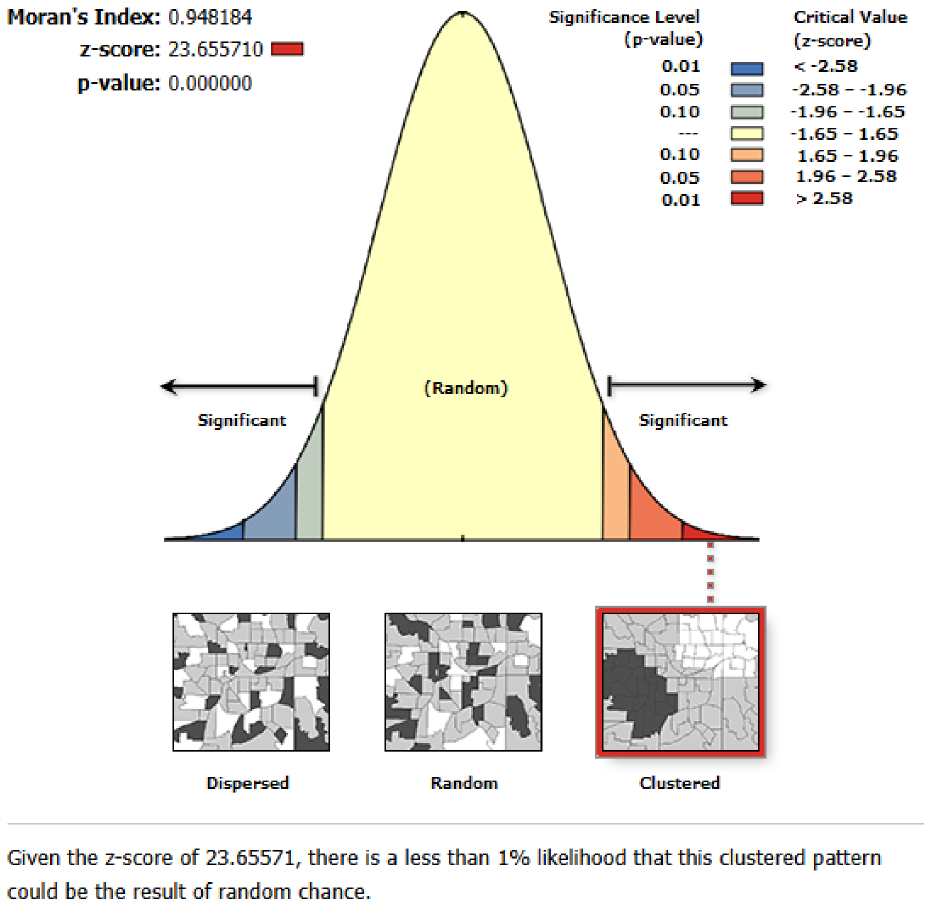

Fig. 15. Global spatial autocorrelation of persistent *S. alterniflora* patches in 2025 based on Global Moran's I. Kernel density of persistent *S. alterniflora* patches in the intertidal zone of DMNNR in 2025.The Moran's I value of 0.95 ($z = 23.66$, $p < 0.001$) indicates a highly clustered spatial pattern of persistent patches within the intertidal study area.

The kernel density surface shows that remnant patches are concentrated in three discrete hotspots along the seaward fringe of the study area **(Fig. 16)**. In the northern section of the DMNNR intertidal zone (inset A), persistent patch density is very high near the outer edge of the former *S. alterniflora* belt, forming two contiguous clusters. A second hotspot is located in the central part of the study area (inset B), where medium to high densities occur along a narrow coastal strip. A third hotspot appears near the southern tip of the study area (inset C), with medium to high densities adjacent to the southernmost seawall segment. Areas between these hotspots show low or near-zero density, indicating that almost no persistent patches remain in large parts of the intertidal flat.

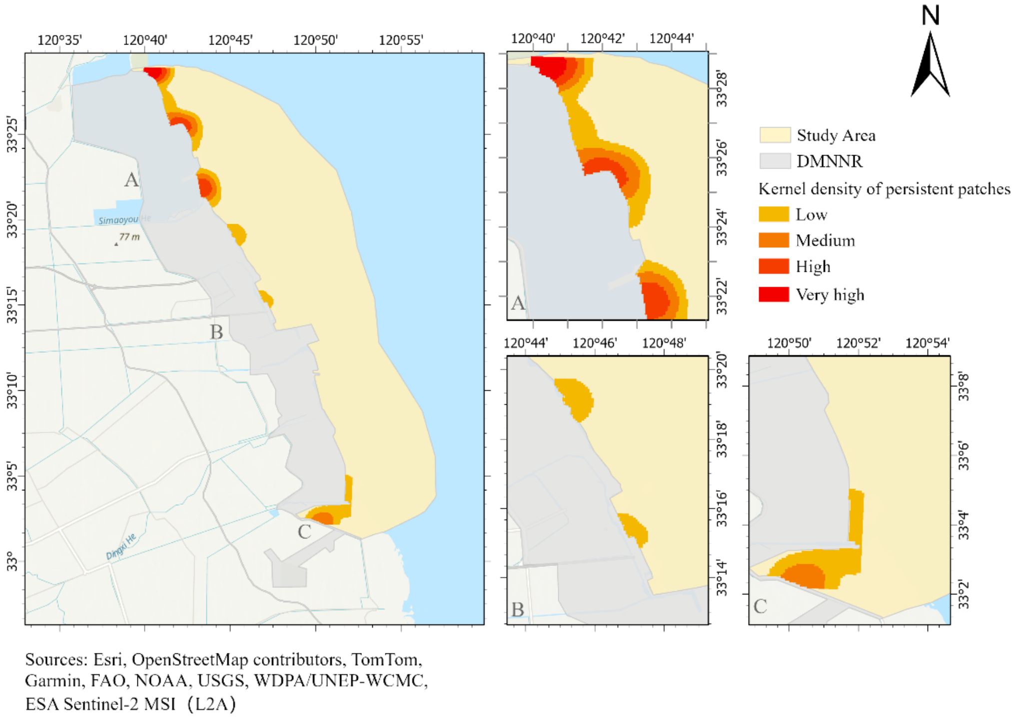

Fig. 16. Kernel density of persistent *S. alterniflora* patches in the intertidal zone of DMNNR in 2025. The main panel shows the kernel density surface across the study area, while insets A–C provide zoomed views of the three main hotspots (very high and high densities) along the seaward fringe of the intertidal zone.

Visual comparison with tidal channels and the DMNNR boundary suggests that persistent hotspots tend to occur close to major channel mouths and along the external margin of the former *S. alterniflora* zone. This spatial pattern indicates that eradication was likely more difficult in zones with complex tidal hydrodynamics or restricted physical access, and highlights these hotspots as priority areas for post-control monitoring and targeted follow-up management.

5. Discussion

5.1. Control Effectiveness

The results of this study indicate that the national *Spartina alterniflora* eradication program implemented in DMNNR from 2022 to 2025 has almost completely removed the species from the reserve. The total area of *S. alterniflora* decreased from 3147.86 ha in December 2022 to 22.84 ha in December 2025, with an overall removal rate of

99.27% and a net reduction of 3125.02 ha. Among the areas identified in 2022, 99.81% (3141.92 ha) had been successfully cleared by 2025, although 16.89 ha of new patches were detected. This outcome greatly exceeds the national target of removing more than 90% of the invaded area by 2025, suggesting that the project can be considered a highly successful example of large-scale management.

Compared with previous regional cases, such as the Chongming Island project reported by Zhang et al. (2020), where substantial residual patches still remained five years after the initial removal in 2013, the performance in DMNNR is significantly more effective. Although some persistent patches remain, they show clear spatial clustering, which provides an opportunity for targeted management to maintain the current control results.

From an ecological perspective, the restoration of approximately 3145 ha of intertidal mudflats represents a significant recovery of critical habitat along the Yellow Sea migratory route. These habitats are essential for migratory shorebirds, which rely on benthic invertebrates exposed during low tide as their main food source (Mu & Wilcove, 2020). Therefore, the near-complete removal of *S. alterniflora* in DMNNR directly supports the conservation goals of this World Natural Heritage Site and contributes to maintaining the ecological integrity of the East Asian–Australasian Flyway (EAAF).

5.2. Residual Patches

The spatial distribution of the remaining *S. alterniflora* in 2025 is not random. Instead, these residual patches show a strong clustering pattern, which is supported by a high Global Moran's I value of 0.95 ($p < 0.001$). The kernel density analysis further identifies three clear hotspot areas located in the northern, central, and southern parts of the study area. This obvious clustering suggests that the incomplete removal of *S. alterniflora* is not due to random processes or general limitations of the management strategy, but is more likely related to local environmental conditions.

There are two possible explanations for the presence and clustering of these residual patches. First, *S. alterniflora* has a strong ability to spread through water, and tidal flow is a key mechanism for dispersal in intertidal environments (Xia et al., 2021). The spatial pattern of newly emerged patches shows that some reinvasion occurs near the edges of previously existing patches, especially along tidal creeks. These areas may receive propagules, such as seeds or plant fragments, from populations outside the reserve, which are then transported into the study area by tidal currents. Second, some areas that are frequently inundated are difficult for mechanical removal equipment to access, or the flooding-based control methods may not be sufficient to completely eliminate the plants. Currently, physical methods such as mowing and enclosed flooding are widely used in coastal wetlands in China, mainly to avoid the environmental risks associated with chemical herbicides (Min et al., 2025). However, in areas with long-term waterlogging, or where cut plants are not submerged for a sufficient period, *S. alterniflora* may regrow from underground rhizomes.

At the same time, the clustered distribution of residual patches can also be advantageous for management. It allows managers to focus on specific hotspot areas, rather than conducting large-scale surveys across the entire intertidal zone. The hotspot map produced in this study can directly support field teams by guiding them to key locations, helping to reduce survey effort and improve efficiency in detecting and removing remaining patches.

5.3. Methodological Strengths and Reliability

The combination of supervised Random Forest (RF) classification and SAI threshold extraction can effectively address a key issue in post-management monitoring. When sufficient training samples are available in the early stage of management, it ensures the reliability of baseline mapping. In the later stage, when residual patches are too sparse to obtain effective samples, it can still achieve results with relatively high confidence, allowing comparison between pre- and post-management conditions.

5.3.1. Complementarity of RF and SAI Methods

In 2022, RF classification achieved an overall accuracy of 94.97% with a Kappa coefficient of 0.924, and producer's and user's accuracies for *S. alterniflora* exceeding 92%. When the SAI threshold method ($-0.790 \leqslant \text{SAI} \leqslant -0.388$ AND $0.275 \leqslant \text{NDVI} \leqslant 0.650$) was applied to the same imagery, the area difference between the two methods was only 4.57% (137.55 ha), and the spatial Intersection over Union (IoU) reached 0.916. This high agreement demonstrates that the SAI threshold is both theoretically grounded in the spectral behavior of senescent *S. alterniflora* (Zuo et al., 2025) and empirically validated against independent supervised classification within the study area. The dual-method validation in 2022 provides a robust benchmark that supports applying the SAI threshold unchanged to 2025 imagery, addressing a key limitation in previous control studies where lack of post-eradication samples precluded quantitative accuracy assessment (Zhang et al., 2020).

5.3.2. Applicability of SAI Threshold in 2025

Three lines of evidence support the continued validity of the SAI threshold in 2025. First, pixels identified as *S. alterniflora* in 2025 exhibit spectral signatures consistent with senescent vegetation in the false-color composite. Second, the SAI and NDVI histograms provide strong evidence of near-complete eradication: the 2022 SAI distribution showed a distinct negative peak at −0.70 corresponding to *S. alterniflora*, which completely disappeared by 2025, with pixel counts below −0.45 reduced to near zero. Similarly, the 2022 NDVI vegetation peak at 0.50–0.55 was entirely absent in 2025. Third, the high spatial clustering of remnant patches (Moran's I = 0.95) in three discrete hotspots suggests genuine ecological patterns rather than classification artifacts.

5.3.3. Attribution of Change to Management Actions

The observed reduction of 3,125.02 ha (99.27%) can be confidently attributed to the 2022–2025 national eradication campaign rather than alternative drivers, based on the following evidence:

Phenological consistency: Both images were acquired in mid-December during the *S. alterniflora* senescence period under low-tide conditions, ensuring that observed differences reflect vegetation change rather than seasonal or tidal variability.

Climate-driven dieback ruled out: *S. alterniflora* is a robust perennial that has persisted in Yancheng for decades (Yan et al., 2021). No large-scale natural dieback events in Jiangsu Province during 2022–2025 have been documented, and no climatic mechanism could plausibly cause 99% area loss within three years. Visual inspection of historical Sentinel-2 imagery for 2023–2024 reveals extensive areas of standing water and visible linear patterns indicative of enclosure-induced flooding and mowing operations features absent from 2022 imagery.

Classification error insufficient: The 2022 RF classification achieved 94.97% overall accuracy, and SAI-RF agreement (IoU = 0.916) confirms consistent identification of *S. alterniflora*. Moreover, the complete disappearance of the SAI peak at −0.70 in the frequency distribution cannot be produced by random classification error.

These multiple independent lines of evidence strongly support the conclusion that the net reduction of 3,125.02 ha is primarily attributable to the 2022–2025 national control campaign.

5.4. Limitations of this study

Several methodological limitations should be acknowledged when interpreting the results of this study.

5.4.1. Lack of independent field validation for 2022 baseline

The 640 reference samples used in this study to train and validate the RF classifier as well as to determine the SAI threshold range were all derived from multi-source image interpretation, rather than from independent field surveys or aerial data. This approach may introduce a "circular validation" problem, because the same samples used for classification are also used to define the reference labels. However, two factors somewhat mitigate this issue. First, this study used three independent data sources (Sentinel-2, CM-SSM 2020, and Google Earth) for validation, which reduces the likelihood of systematic mislabeling. Second, the sampling process deliberately covered the full range of spectral variation, including high-density core areas, sparse patches, and edge transition pixels, so that the training data could represent as many land cover types as possible. Nevertheless, because of the lack of independent ground-truth validation samples, the reported overall accuracy of 94.97% in 2022 should be regarded as an overestimated value. If independent field validation data were available, the actual accuracy might be lower.

5.4.2. Absence of independent validation for 2025

No field surveys were conducted in 2025, so the post-management classification results could not be formally validated for accuracy. As a result, the reliability of the 2025 results mainly depends on the indirect evidence mentioned earlier. Although these lines of evidence mentioned before collectively support the conclusion that *S.alterniflora* has been largely removed, the lack of quantitative accuracy metrics means that the 2025 results still carry some uncertainty, especially regarding the exact area and spatial location of the residual patches, where errors may persist.

5.5. Implications for Future Monitoring and Management

S. alterniflora was almost completely removed from DMNNR by December 2025, marking a shift in management priority from large-scale eradication to long-term prevention of reinvasion. The corresponding monitoring strategy should also be adjusted, moving from full-coverage mapping of extensive invaded areas to targeted monitoring of small residual and newly emerging patches.

First, for DMNNR, an annual Sentinel-2 image from December can be used to quickly identify potential *S. alterniflora* patches by directly reapplying the pre-defined SAI thresholds without collecting new training samples. These areas can then be examined using high-resolution drone imagery to confirm species identity and define precise boundaries. This creates a “satellite–drone” synergistic monitoring system that improves detection efficiency.

Second, for other study areas, this study provides a transferable workflow: (i) collect reference samples through multi-source image interpretation (historical products, Google Earth, and Sentinel-2 composites); (ii) apply a Random Forest classifier to derive area-specific SAI thresholds; (iii) validate the reliability of these thresholds using the agreement between RF and SAI (measured by Intersection-over-Union); and (iv) directly apply the validated thresholds to post-removal images without new training samples. Because post-management samples are often difficult to obtain (due to restricted access to some protected areas or to the small number of remaining patches after control), this workflow is valuable for the current national-scale *S. alterniflora* eradication program.

6. Conclusions

This study quantitatively assessed the effectiveness of the 2022–2025 national *Spartina alterniflora* control campaign in Dafeng Milu National Nature Reserve (DMNNR) using Sentinel-2 imagery and a dual-method mapping framework combining Random Forest classification with SAI threshold extraction. Three key findings emerge from the analysis.

First, the control campaign achieved near-complete eradication of *S. alterniflora* within the DMNNR intertidal zone. The invaded area declined from 3,147.86 ha in December 2022 to 22.84 ha in December 2025, representing an eradication rate of 99.27% and a net removal of 3,125.02 ha. This outcome substantially exceeds the national target of >90% removal. The restoration of over 3,000 ha of unvegetated tidal flat directly supports the conservation objectives of the UNESCO World Heritage site "Migratory Bird Sanctuaries along the Coast of Yellow Sea–Bohai Gulf of China" and contributes to maintaining critical foraging habitat for globally threatened shorebird species dependent on the East Asian–Australasian Flyway.

Second, remnant *S. alterniflora* patches exhibit strong spatial clustering rather than random distribution. Spatial autocorrelation analysis revealed a Global Moran's I value of 0.95 ($p < 0.001$), and kernel density estimation identified three discrete hotspot areas in the northern, central, and southern sections of the reserve. These persistent and newly established patches are concentrated along the seaward fringe of the study area, suggesting that external propagule pressure from adjacent invaded coastlines and localized constraints on physical removal effectiveness are the primary drivers of incomplete eradication. The clustered distribution pattern provides a practical basis for targeted follow-up monitoring and removal, enabling field teams to prioritize spatially explicit management actions in 2026 and subsequent years to prevent reinvasion.

Third, the dual-method validation framework developed in this study provides a transferable and scalable approach for post-eradication monitoring in coastal reserves where field access is constrained. The high spatial agreement between RF and SAI results in 2022 (IoU = 0.916), combined with multiple lines of spectral evidence supporting the reliability of the 2025 extraction, demonstrates that this approach can produce consistent and defensible change estimates across years. The validation workflow, rather than the specific threshold values, is directly applicable to other coastal reserves implementing the national *S. alterniflora* control program, providing a standardized tool for regional and national-scale evaluation.

However, important limitations must be acknowledged. The reference samples used to train and validate the 2022 baseline map were derived from multi-source image interpretation rather than independent field surveys, and no ground-truth validation data were collected in 2025. Future monitoring efforts should incorporate targeted UAV surveys and field validation at the identified hotspot areas to confirm patch identity and refine management strategies.

In conclusion, this study demonstrates that the 2022–2025 national control campaign has been highly effective in DMNNR, achieving near-complete removal of *S. alterniflora* and restoring the ecological integrity of the intertidal zone. The spatially explicit distribution maps and clustered pattern of remnant patches provide actionable information for priority management areas, while the transferable dual-method framework offers a useful tool for evaluating control effectiveness across the broader network of coastal reserves participating in the national eradication program.

References

Belgiu, M., & Drăguţ, L. (2016). Random forest in remote sensing: A review of applications and future directions. ISPRS Journal of Photogrammetry and Remote Sensing, 114, 24–31. https://doi.org/10.1016/j.isprsjprs.2016.01.011

Breiman, L. Random Forests. *Machine Learning* **45**, 5–32 (2001). https://doi.org/10.1023/A:1010933404324

Chan, Y.-C., Peng, H.-B., Han, Y.-X., Chung, S. S.-W., Li, J., Zhang, L., & Piersma, T. (2019). Conserving unprotected important coastal habitats in the Yellow Sea: Shorebird occurrence, distribution and food resources at Lianyungang. *Global Ecology and Conservation, 20*, e00724. https://doi.org/10.1016/j.gecco.2019.e00724

Chen, Q., Shen, C., Du, H., & Tang, D. (2025). Comparing supervised classification algorithm–feature combinations for *Spartina alterniflora* extraction: A case study in Zhanjiang, China. Frontiers in Remote Sensing, 6, 1606549. https://doi.org/10.3389/frsen.2025.1606549

Congalton, R. G. (1991). A review of assessing the accuracy of classifications of remotely sensed data. *Remote Sensing of Environment, 37*(1), 35–46. https://doi.org/10.1016/0034-4257(91)90048-B

Davies, B. F. R., Gernez, P., Geraud, A., Oiry, S., Rosa, P., Zoffoli, M. L., & Barillé, L. (2023). Multi- and hyperspectral classification of soft-bottom intertidal vegetation using a spectral library for coastal biodiversity remote sensing. Remote Sensing of Environment, 297, 113554. https://doi.org/10.1016/j.rse.2023.113554

Dong, D., Huang, H., & Gao, Q. (2024). Tracking the Dynamics of *Spartina alterniflora* with WorldView-2/3 and Sentinel-1/2 Imagery in Zhangjiang Estuary, China. Water, 16(13), 1780. https://doi.org/10.3390/w16131780

Duan, Y., Sanchez-Azofeifa, A., Chen, C., Tian, B., Li, X., Sengupta, D., & Zhou, Y. (2026). S2Coast-2023: The first global 10-meter resolution coastline dataset derived from enhanced Sentinel-2 composite imagery using Google Earth Engine. *Remote Sensing of Environment, 334*, 115186. https://doi.org/10.1016/j.rse.2025.115186

Foody, G. M. (2002). Status of land cover classification accuracy assessment. Remote Sensing of Environment, 80(1), 185–201. https://doi.org/10.1016/S0034-4257(01)00295-4

Hengl, T., Nussbaum, M., Wright, M. N., Heuvelink, G. B. M., & Gräler, B. (2018). Random forest as a generic framework for predictive modeling of spatial and spatio-temporal variables. PeerJ, 6, e5518. https://doi.org/10.7717/peerj.5518

IUCN. (2021). *World Heritage Outlook: Migratory Bird Sanctuaries along the Coast of Yellow Sea–Bohai Gulf of China*. International Union for Conservation of Nature. https://worldheritageoutlook.iucn.org/explore-sites/migratory-bird-sanctuaries-along-coast-yellow-sea-bohai-gulf-china

Jiang, Y., Yang, D., Huang, J., Wen, Y., Tang, H., Xu, J., Lin, X., Sun, D., & Gao, D. (2024). Invasive *Spartina alterniflora* alters sediment organic carbon mineralization dynamics in a coastal wetland of southeastern China. *Frontiers in Marine Science, 11*, 1400381. https://doi.org/10.3389/fmars.2024.1400381

Kim, S., Yu, C., Ruesink, J., & Hong, J.-S. (2023). Vertical distribution of the salt marsh invader *Spartina alterniflora* and native halophytes on the west coast of Korea in relation to tidal regimes. Aquatic Invasions, 18(3), 331–349. https://doi.org/10.3391/ai.2023.18.3.104556

Lechner, A. M., Stein, A., Jones, S. D., & Ferwerda, J. G. (2009). Remote sensing of small and linear features: Quantifying the effects of patch size and length, grid position and detectability on land cover mapping. *Remote Sensing of Environment, 113*(11), 2518–2529. https://doi.org/10.1016/j.rse.2009.06.002

Lee, W. G. (2013). Introduced plants, negative effects of. In S. A. Levin (Ed.), Encyclopedia of biodiversity (2nd ed.). Academic Press. https://doi.org/10.1016/B978-0-12-384719-5.00076-9

Liu, H., Cui, G., Zhao, S., Huang, X., Wang, Q., Zhao, C., Jia, M., Yu, H., Wang, Z., & Li, H. (2025). Assessment of *Spartina alterniflora* management effectiveness in Shandong Province based on phenological features and deep learning models. IEEE Journal of Selected Topics in Applied Earth Observations and Remote Sensing, 18, 27000–27011. https://doi.org/10.1109/JSTARS.2025.3618846

Ma, Z., Choi, C.-Y., Gan, X., Li, J., Liu, Y., Melville, D. S., Mu, T., Piersma, T., & Zhang, Z. (2023). Achievements, challenges, and recommendations for waterbird conservation in China's coastal wetlands. Avian Research, 14, 100123. https://doi.org/10.1016/j.avrs.2023.100123

Melville, D. S., Chen, Y., & Ma, Z. (2016). Shorebirds along the Yellow Sea coast: Use of intertidal habitats and implications for conservation. *Emu – Austral Ornithology, 116*(2), 120–129. https://doi.org/10.1071/MU15045

Min, Y., Ke, Y., Zhuo, Z., Qi, W., Li, J., Li, P., & Zhao, N. (2025). Monitoring *Spartina alterniflora* removal dynamics across coastal China using time series Sentinel-1 imagery. *Remote Sensing of Environment, 309*, 114813. https://doi.org/10.1016/j.rse.2025.114813

Moussaid, A., Bayad, M., Gamoussi, Y., El Hamdouni, Y., & Briak, H. (2026). K-means clustering applied to vegetation indices for mapping cultivated areas using high-resolution Moroccan Mohammed VI satellite imagery. Scientific Reports, 16, 11040. https://doi.org/10.1038/s41598-026-41167-1

National Forestry and Grassland Administration. (2022). Special action plan for *Spartina alterniflora* prevention and control (2022–2025) (Wetland Management Department Circular No. 132). Retrieved from http://www.forestry.gov.cn/

Mu, T., & Wilcove, D. S. (2020). Upper tidal flats are disproportionately important for the conservation of migratory shorebirds. *Proceedings of the Royal Society B: Biological Sciences, 287*(1928), 20200278. https://doi.org/10.1098/rspb.2020.0278

Nie, M., Liu, W., Pennings, S. C., & Li, B. (2022). Lessons from the invasion of *Spartina alterniflora* in coastal China. *Ecology, 103*(12), e3874. https://doi.org/10.1002/ecy.3874

Ouyang, Z. T., Gao, Y., Xie, X., Guo, H. Q., Zhang, T. T., & Zhao, B. (2013). Spectral discrimination of the invasive plant *Spartina alterniflora* at multiple phenological stages in a saltmarsh wetland. PLOS ONE, 8(6), e67315. https://doi.org/10.1371/journal.pone.0067315

Roberts, D. R., Bahn, V., Ciuti, S., Boyce, M. S., Elith, J., Guillera-Arroita, G., Hauenstein, S., Lahoz-Monfort, J. J., Schröder, B., Thuiller, W., Warton, D. I., Wintle, B. A., Hartig, F., & Dormann, C. F. (2017). Cross-validation strategies for data with temporal, spatial, hierarchical, or phylogenetic structure. *Ecography, 40*(8), 913–929. https://doi.org/10.1111/ecog.02881

Seger, K. D., Sousa-Lima, R., Schmitter-Soto, J. J., & Urban, E. R. Jr. (2021). Editorial: Before-After Control-Impact (BACI) studies in the ocean. *Frontiers in Marine Science*, 8, Article 787959. https://doi.org/10.3389/fmars.2021.787959

Song, S., Wu, Z., Wang, Y., Cao, Z., He, Z. and Su, Y. (2020) Mapping the Rapid Decline of the Intertidal Wetlands of China Over the Past Half Century Based on Remote Sensing. Front. Earth Sci. 8:16. https://doi.org/10.3389/feart.2020.00016

Stock, A. (2025). Choosing blocks for spatial cross-validation: Lessons from a marine remote sensing case study. *Frontiers in Remote Sensing, 6*, 1531097. https://doi.org/10.3389/frsen.2025.1531097

UNESCO. (2019). *Migratory Bird Sanctuaries along the Coast of Yellow Sea–Bohai Gulf of China (Phase I)* (World Heritage List, Decision 43 COM 8B.3). UNESCO World Heritage Centre. https://whc.unesco.org/en/decisions/7358

Wang, C., Wang, G., Dai, L., Liu, H., Li, Y., Qiu, C., Zhou, Y., Chen, H., Dong, B., Zhao, Y., & Zhang, Y. (2021). Study on the effect of habitat function change on waterbird diversity and guilds in Yancheng coastal wetlands based on structure–function coupling. *Ecological Indicators*, 119, 107223. https://doi.org/10.1016/j.ecolind.2020.107223

Wulder, M. A., Franklin, S. E., White, J. C., Linke, J., & Magnussen, S. (2006). An accuracy assessment framework for large-area land cover classification products derived from medium-resolution satellite data. *International Journal of Remote Sensing, 27*(14), 2981–3000. https://doi.org/10.1080/01431160500185284

Xia, S., Wang, W., Song, Z., Kuzyakov, Y., Guo, L., Van Zwieten, L., Li, Q., Hartley, I. P., Yang, Y., Wang, Y., … Wang, H. (2021). *Spartina alterniflora* invasion controls organic carbon stocks in coastal marsh and mangrove soils across tropics and subtropics. *Global Change Biology, 27*(8), 1627–1644. https://doi.org/10.1111/gcb.15516

Yan, D., Li, J., Xie, S., Liu, Y., Sheng, Y. and Luan, Z. (2022) Examining the expansion of *Spartina alterniflora* in coastal wetlands using an MCE-CA-Markov model. Front. Mar. Sci. 9:964172. https://doi.org/10.3389/fmars.2022.964172

Yan, D., Li, J., Yao, X., & Luan, Z. (2021). Quantifying the long-term expansion and dieback of *Spartina alterniflora* using Google Earth Engine and object-based hierarchical random forest classification. IEEE Journal of Selected Topics in Applied Earth Observations and Remote Sensing, 14, 9781–9793. https://doi.org/10.1109/JSTARS.2021.3114116

Yao, H., Chen, M., Huang, Z., Huang, Y., Wang, M., & Liu, Y. (2024). Remote sensing monitoring and potential distribution analysis of *Spartina alterniflora* in coastal zone of Guangxi. *Ecology and Evolution, 14*(6), e11469. https://doi.org/10.1002/ece3.11469

Zhang, X., Jia, M., Yan, F., Zhang, Y., Man, W., Li, F., Liu, M., Wu, F., Yin, X., & Duan, J. (2025). Advancing coastal wetland management: A combined UAV–satellite approach for *Spartina alterniflora* aboveground biomass estimation using interpretable machine learning. *International Journal of Digital Earth, 18*(x), 2525383. https://doi.org/10.1080/17538947.2025.2525383

Zhang, X., Xiao, X., Wang, X., Xu, X., Chen, B., Wang, J., Ma, J., Zhao, B., & Li, B. (2020). Quantifying expansion and removal of *Spartina alterniflora* on Chongming Island, China, using time series Landsat images during 1995–2018. *Remote Sensing of Environment*, 247, 111916. https://doi.org/10.1016/j.rse.2020.111916

Zheng, J., Wei, H., Chen, R., Liu, J., Wang, L., & Gu, W. (2023). Invasive trends of *Spartina alterniflora* in the southeastern coast of China and potential distributional impacts on mangrove forests. *Plants, 12*(10), 1923. https://doi.org/10.3390/plants12101923

Zheng, X., Javed, Z., Liu, B., Zhong, S., Cheng, Z., Rehman, A., Du, D., & Li, J. (2023). Impact of *Spartina alterniflora* invasion in coastal wetlands of China: Boon or bane? *Biology*, 12(8), 1057. https://doi.org/10.3390/biology12081057

Zhou, B., Xu, M., Tian, J., Jia, M., Mao, D., Cheng, K., Zhu, X., Jiang, H., Song, J., Ke, Y., Zhang, Z., Huang, Y., Wei, M., Zhu, L., Li, X., and Gong, H.: National-scale sub-meter mapping of *Spartina alterniflora* in mainland China 2020, Earth Syst. Sci. Data, 17, 6601–6620. https://doi.org/10.5194/essd-17-6601-2025

Zuo, Y., Yang, G., Sun, W., Huang, K., Yang, S., Chen, B., Wang, L., Meng, X., Wang, Y., Li, J., & others. (2025). SAI: A *Spartina alterniflora* index based on Sentinel-2 multispectral imagery for *Spartina alterniflora* mapping. Journal of

Remote Sensing, 5, 0510. https://doi.org/10.34133/remotesensing.0510